CHALMERS

Path Control Algorithms for Autonomous Steering and Braking of Heavy Vehicles

-Intended for Severe Rear-end Collision Avoidance Manoeuvres

Master's Thesis in the Automotive Engineering Master's Programme

ÖDÜL BIRGE BILEN

Department of Applied Mechanics
Division of Vehicle Engineering and Autonomous Systems
CHALMERS UNIVERSITY OF TECHNOLOGY
Göteborg, Sweden 2010
Master's Thesis 2010:59

MASTER'S THESIS 2010:59

Path Control Algorithms for Autonomous Steering and Braking of Heavy Vehicles

-Intended for Severe Rear-end Collision Avoidance Manoeuvres

Master's Thesis in the Automotive Engineering Master's Programme

ÖDÜL BIRGE BILEN

Department of Applied Mechanics
Division of Vehicle Engineering and Autonomous Systems
CHALMERS UNIVERSITY OF TECHNOLOGY
Göteborg, Sweden 2010

Path Control Algorithms for Autonomous Steering and Braking of Heavy Vehicles
-Intended for Severe Rear-end Collision Avoidance Manoeuvres
Master's Thesis in the Automotive Engineering Master's Programme
ÖDÜL BIRGE BILEN

© ÖDÜL BIRGE BILEN, 2010

Master's Thesis 2010:59
ISSN 1652-8557
Department of Applied Mechanics
Division of Vehicle Engineering and Autonomous Systems
Chalmers University of Technology
SE-412 96 Göteborg
Sweden
Telephone: + 46 (0)31-772 1000

Chalmers Reproservice/Department of Applied Mechanics
Göteborg, Sweden 2010

Path Control Algorithms for Autonomous Steering and Braking of Heavy Vehicles
-Intended for Severe Rear-end Collision Avoidance Manoeuvres
Master's Thesis in the Automotive Engineering Master's Programme
ÖDÜL BIRGE BILEN
Department of Applied Mechanics
Division of Vehicle Engineering and Autonomous Systems
Chalmers University of Technology

ABSTRACT

In this study, path control algorithms for autonomous steering and braking interventions intended for severe rear-end collision avoidance manoeuvres of heavy vehicles are evaluated with computer simulations.

First of all, in order to acquire basic kinematical data for the driving conditions prior to an accident, an accident database search was carried out using the ETAC (European Truck Accident Causation) database with the focus on three variants of rear-end collisions (due to a stopped vehicle in front, a slowing vehicle in front and a slow vehicle in front travelling at constant speed) for the thesis work. The travel speeds for the host and the target vehicles before the crash as well as basic road details were obtained. Because of simple nature of the rear-end collisions due to stopped vehicle in front, this was chosen as the accident of interest for this study.

Secondly, different possible closed-loop path control algorithms utilising either steering or differential braking were designed. The steering controllers proposed in this study are either proportional (P) or proportional-derivative (PD) type control. For the differential brake control, only a proportional controller was proposed. All these controllers were tailored to include what is called prediction distance and they were integrated for possible alignments of the truck with respect to the desired escape path.

Thirdly, all proposals in control algorithms were tested with a four degree-of-freedom truck model using numerical computer simulations. For development purposes, a severe path resembling the escape path of the accidents scenario of interest was designed. The effect of control parameters and the prediction distance on the path following performance were evaluated. The implementation of a prediction distance was found to help the control algorithm to keep the truck on the desired path with lesser lateral deviations and better stability.

Finally, the entire set of control parameters and the prediction distance that had been found to perform well were combined and tested for a realistic collision avoidance manoeuvre which was almost in the absolute limit of wheel lift-off for the heavy vehicle. It was seen that reduction of speed was necessary for the vehicle to be able to follow the path with minimal lateral deviations and without wheel lift-off. For this reason, open-loop application of soft service braking throughout the manoeuvre was investigated and it was found that path control performance had increased.

Key words: path control, autonomous steering and braking, heavy vehicles, active safety

Contents

Preface

This work has been conducted at Chalmers University of Technology as a part of EU research project “interactIVe” within the Seventh Framework Programme. Therefore, I would like to thank EU Commission and Chalmers University of Technology for the financial support and for their determination towards safe transportation.

In addition, I am personally indebted to:

- Mathias Lidberg, from Vehicle Engineering and Autonomous Systems Division at Chalmers, for supervising this project and for being more than a supervisor in everything else. I am also grateful to him for being a gentle boss.

- Helen Fagerlind, from SAFER Research Centre at Chalmers, for her immense assistance in accident database search and for her patience with me. Without her invaluable help, I would never be able to do it by myself.

- Matias Viström, from SAFER Research Centre at Chalmers, for his contribution to the accident database search in his busy schedule.

- Thomas Englund, Agneta Sjögren and Lars Bjelkeflo; from Volvo Technology, for productive discussions particularly on the path control hardware and the strategies.

- Johan Engström, from Volvo Technology, for his contribution in accident database search and for his help in getting access to the database.

- Ulrich Sander, from Autoliv, for his voluntary help in providing solutions to the error messages I was continuously receiving while working on the database tool.

- All of my instructors at Istanbul Technical University and Chalmers University of Technology for their endeavours in conveying engineering knowledge and notion.

- My family, for their infinite support and encouragement whenever I felt depressed.

Göteborg, November 2010

Ödül Birge Bilen

Notations

Note: Some of these notations appear as a subscript in the thesis work.

Roman upper case letters

B	Stiffness factor (Magic Formula), width, trackwidth
C	Stiffness (mainly for cornering), shape factor (Magic Formula), coefficient (mainly for cornering stiffness vs. normal load), damping (mainly for roll)
D	Peak value (Magic Formula)
E	Curvature factor (Magic Formula)
F	Tyre force
I	Mass moment of inertia
K	Stiffness (mainly for roll), controller gain
L	Length (with a subscript), distance between the first and the second axles (without a subscript), wheelbase (with a subscript)
R	Radius of curvature
S	Curve length
X	Longitudinal direction in earth fixed coordinate system
Y	Lateral direction in earth fixed coordinate system
Z	Vertical direction in earth fixed coordinate system

Roman lower case letters

a	Asymptote (mainly for horizontal), acceleration
c	Compliance
d	Differential (mainly for controller gain), prediction distance
g	Gravitational acceleration
h	Height (with a superscript), roll centre height from the ground (with a subscript), CG height (without a subscript)
i	The number of a particular axle, mechanical gain (with a subscript)
l	Distance between two reference points
m	Maximum (or corresponding to the maximum), mass (with a subscript), total mass of the truck (without a subscript)
n	The number of a particular wheel (or wheel system for dual wheels)
p	Proportional (mainly for controller gain)
s	Steering system (mainly for mechanical gain or ratio of the steering system)
t	Theoretical (mainly for wheelbase), time
v	Velocity
w	Maximum lateral displacement in the desired escape path
x	Longitudinal direction in vehicle fixed coordinate system
y	Lateral direction in vehicle fixed coordinate system
z	Vertical direction in vehicle fixed coordinate system

Greek lower case letters

α	Tyre slip angle

δ	Steering angle (also used as a subscript indicating the whole steering system)
ε	Roll steer coefficient
ϕ	Roll angle of the sprung mass
μ	Adhesion coefficient between the road and the tyre, coefficient (mainly for adhesion coefficient vs. normal load)
σ	Tyre relaxation length, standard deviation
τ	Time constant for a first order system
ψ	Yaw angle of the vehicle

Short indicators

brake	Brake system, braking (mainly for service braking or differential braking)
BS	Bogie spread
control	Controlled (or demanded by the control system)
filter	Low-pass filter
fo	Front overhang
in	Inner
initial	Initial value
lim	limit value
mf	Steady state value calculated from Magic Formula
max	Maximum (mainly for the geometric limits of the vehicle)
net	Net (mainly for the steering angles after kinematics and elastokinematics)
new	The new physical quantity with prediction distance applied
out	Outer
ref	Reference (mainly for escape path), nominal value
rim	Wheel rim (or circumference of wheel rim)
ro	Rear overhang
spr	Sprung (mainly for mass)
ss	Steady state
stat	Static
SWA	Steering wheel angle
tandem	Tandem axle group
tot	Total (mainly for tyre force in particular direction)
unspr	Unsprung (mainly for mass)

Superscript

$'$ (prime)	From roll axis to the CG (mainly for height)

Acronyms encountered in text and some figures

4WS	Four Wheel Steering
CG	Centre of Gravity
ESP	Electronic Stability Programme
EU	European Union
GPS	Global Positioning System
ISO	International Organization for Standardization
RC	Roll Centre

1 Introduction

Traffic safety is a major problem for today's transportation. A lot of work has been done in the passive safety area where milliseconds after the initiation of crash are of importance; nowadays collision avoidance (or in other words, collision-free traffic) in the field of active safety is more prioritised.

Even though there are numerous definitions of active safety, one should not immediately think of intelligent electronic/mechatronic systems when it is concerned: Active safety relates to everything that prevents accidents from happening [1]. Therefore, it does not only need to be the systems in the vehicles which intervene in the situation when the driver acts incorrectly; it could also be properly designed brake system, well tuned chassis for optimal vehicle dynamics, a headlight system providing good illumination and even proper driver education! However; this study focuses on autonomous path and path stability control of heavy vehicles which may serve as a basis for active interventions, particularly intended for helping the driver in critical collision avoidance manoeuvres. The detailed "Safety Phase Chart" in Figure 1 shows the time sequence of an accident and the region where the active safety and collision avoidance are located in it:

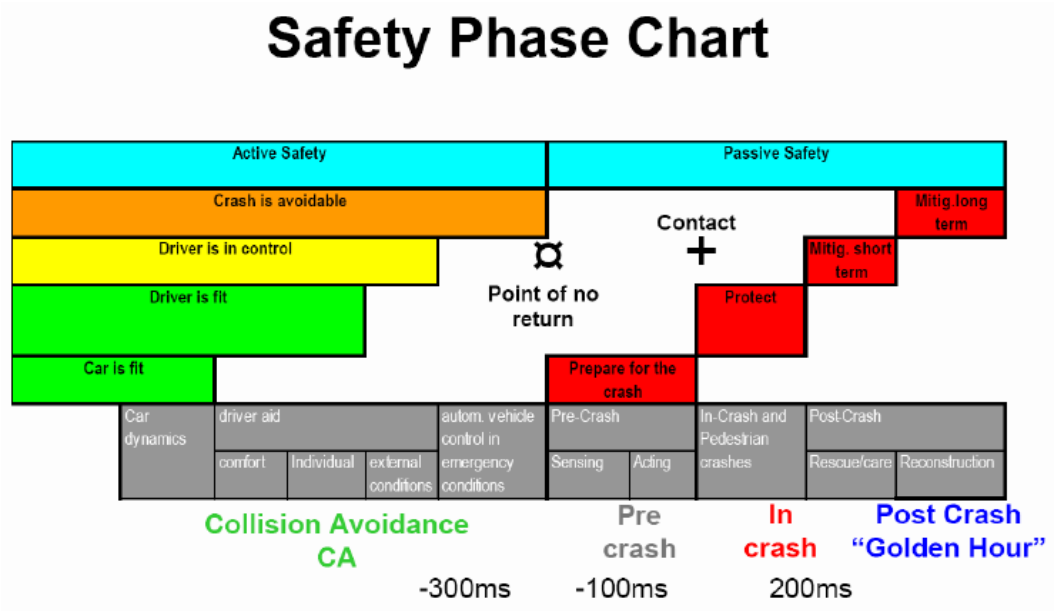

Figure 1 The Safety Phase Chart (Adopted from Ref. [2]).

So far, yaw stability control algorithms (Bosch names it ESP) have been proven to work efficiently. According to Vägverket, ESP is effective in 22% of all accidents and this figure is increasing in the accident types where the surface is slippery [3]. However, the frequency of the remaining accidents is still high. This reveals that it is not enough to control the vehicles for understeer and oversteer to be able to cope with the problems proceeded by accidents. It is essential to avoid two vehicles being on the same coordinate at the same time: This implies that the vehicles should be controlled for a given path!

An average human driver is often helpless in critical driving situations: The driver sometimes reacts late to an imminent crash due to lack of situation awareness or physical limitations. Moreover, because of panic in the situations when the handling limits are reached, driver reaction is usually more than what is required [4]. ESP helps to remedy this; but because the main control is on the driver, it cannot prevent vehicles from being on the same coordinate at the same time.

Pure application of the service brakes to avoid an accident (by stopping the vehicle before colliding with the obstacle in front) is insufficient at high relative speeds. Only differential braking to steer the vehicle away from the obstacle in front is not feasible for a collision avoidance manoeuvre on the limit either; since, if this system is used, the sufficient amount of lateral forces will be built up once the vehicle yaw rate increases up to certain level (in other words, too slow response!). This type of actuation is more suitable for lane keeping purposes, as demonstrated by Nissan [5]. Therefore the steering intervention comes into play in order to avoid accidents where the handling limits of the vehicle should be utilised as much as possible.

1.1 Problem Definition

A very general definition of the problem treated here is the question of how to keep a three-axle-truck autonomously on a desired escape path (on the limits). However, this is too general especially the number of solutions and/or combination of them is concerned; therefore the problem has to be narrowed down. In this study, main focus is on:

- the control algorithm and
- the type of actuation (steering, braking or their integration)

which will make "the path following on the limits" to be realised.

The comparison of service braking and steering in a collision avoidance manoeuvre cannot be easily done when a full vehicle simulation is used. However, a particle model could be used to find out the outer bounds of these two actuation types. The following schematic diagram depicts what happens if a particle model is used to compare steering and braking (constant acceleration level).

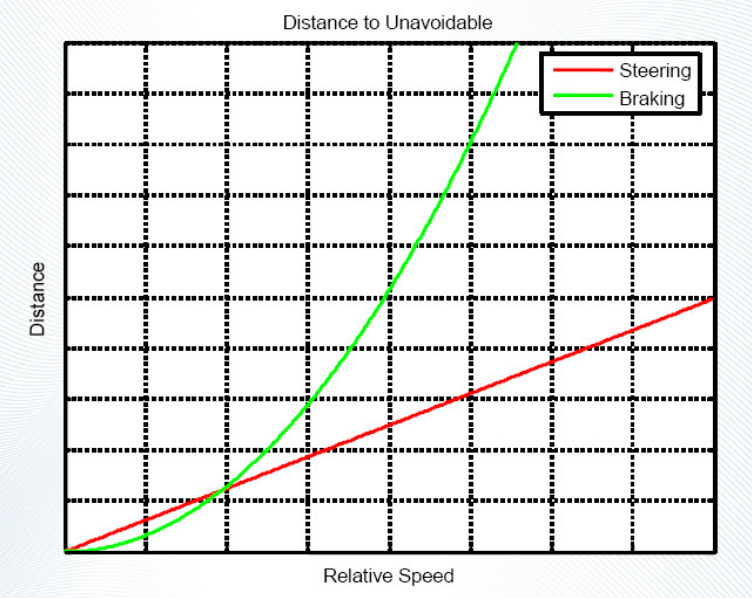

Figure 2 The schematic comparison between steering and braking to avoid an obstacle (Adopted from Ref. [6])

From the Figure 2, it could be concluded that the steering becomes more efficient to use at high relative speeds provided that there is enough lateral space to escape into and the maximum adhesion that could be exploited from the surface is enough to reach the required lateral acceleration. However, there is one more condition for a heavy vehicle, that is, the rollover! The achievable maximum lateral acceleration is subject to the untripped rollover lateral acceleration threshold. This means that steering becomes favourable at even higher speeds. It is also worth to note that this speed may turn out to be higher than a truck could frequently reach; this has to be taken into account when designing a collision avoidance system.

Possible and feasible actuation solutions for this study can be listed as follows:

- Pure front axle steering,
- Front axle steering + braking (differential braking and/or service braking),
- Front axle steering + braking (differential braking and/or service braking) + tag axle steering.

The second option is chosen in this study in order to improve the transient cornering of the truck but at the same time not to increase the complexity of the truck control too much.

It is worth to note that an additional yaw moment (in order to improve yaw stability or counteract understeer) could be exerted on the vehicle by either differential braking or torque vectoring in the case of traction. However, positive longitudinal forces (i.e. tractive forces) increase the speed of the vehicle; therefore it will cast doubt on utilisation of it in an active safety and path following application. Hence, only

negative longitudinal forces (i.e. brake forces) will be used so as to create a yaw moment when needed.

The evaluation criteria for various settings of the controller are given as follows according to the priority:

1. All wheels must remain in contact with the road: This is important to be able to carry out the simulation from the beginning until the end. When wheel lift is detected, simulation has to be aborted because of the reason explained in the tyre model section.

2. The lateral deviation from the reference path at the point where the obstacle is located should be as small as possible: This is important in order not to impact the obstacle as the reference (desired) path is designed so that the vehicle will follow it with small lateral deviations and avoid the obstacle.

3. The maximum path deviation should be as small as possible: This is especially important, for instance, in order for the vehicle not to depart from the road after the obstacle in front has been avoided.

4. The steering control input should be as smooth (i.e. free of vibrations) as possible in order to hand over the control to the driver without a problem.

1.2 Limitations and Assumptions

As in all studies, there are also simplifications, limitations and assumptions in this study as well. Some of them are related to the control system dynamics which are used to simulate the behaviour of the controlled vehicle, whereas the rest is about the vehicle chassis and tyre properties.

1.2.1 Limitations and Assumptions in the Control System Dynamics

- The entire desired path is given in advance.

- Only high μ environment: Simulations on a low μ surface requires a different tyre model.

- Steering actuator delays and dynamics are not modelled.

- The delays due to slack in brake system are ignored. Instead, brake system is assumed to be pre-charged so that the effect of slack in brake performance is minute.

- Analogue brake and steering actuators are assumed in the simulation (i.e. infinite resolution, infinite update frequency).

1.2.2 Limitations and Assumptions in the Vehicle Chassis and Tyre Model

- Pitch dynamics is not modelled. In fact, yaw and roll motion together influence the pitch dynamics due to the gyroscopic effect. Longitudinal load transfer is calculated by assuming a rigid (i.e. suspension locked for pitch motion) vehicle and cross terms consisting of roll, yaw and their rates are not considered.

- Aerodynamic drag and the effect of possible side winds are not modelled.

- Suspension springs and dampers are assumed to behave linearly for the whole range of roll angles and roll rates.

- Elastokinematical features (e.g. lateral force steer and aligning moment steer) of the suspension are not considered when modelling the axles. For all the axles, only the roll steer (i.e. kinematical feature) is taken into consideration with a simple linear expression. The camber change in rigid axles due to roll of sprung mass (lateral load transfer) is relatively small, that is also neglected.

- In a tandem axle group, longitudinal force and torque on one axle (located on the tandem axle) actually influence the vertical load on the other axle due to the measures taken to distribute the load on each axle of the tandem group in a predefined ratio on uneven surfaces (usually scale beam principle is used [7]). Here, it is assumed that the torque reaction rods used to counteract additional vertical load transfer due to torques and longitudinal forces are designed properly so that they (almost) cancel that effect.

- The steering angles of the left and right front wheels (on the first axle) are assumed to be the same. The steering ratio is assumed to be constant (Indeed, this is a very rough approximation!). The lumped elasticity in the steering system is assumed to be linear.

- Ladder chassis is assumed to be rigid. In reality, truck chassis is made of so-called profiles with “open” cross-sections. Since those profiles are torsionally flexible and relatively rigid for bending, the overall chassis structure is easily twisted. This is sometimes desired for trucks to better suit the road profile. However, as can be expected, torsionally flexible ladder chassis affects the lateral load transfer, but its affect on load transfer is not considered.

- Tyre rolling resistance is neglected.

- A linear reduction is assumed for the adhesion coefficient between the tyre and the ground with respect to the increasing normal load. Moreover, the horizontal asymptote for tyre lateral force vs. slip angle characteristic is assumed to be 75% of the peak force (See “Modelling of a heavy truck” section for details).

- A linear change is assumed for the horizontal position of the tyre peak force vs. slip angle point (See “Modelling of a heavy truck” section for details).

- A first order differential equation with constant relaxation length is used to model tyre force build-up.

- Rotating wheels are not simulated in order not to take the combined slip into account. A friction circle is used to determine the lateral force generated by a tyre in presence of a known longitudinal force.

Reader should be aware of the fact that many limitations listed in Sections 1.2.1 and 1.2.2 are the consequences of lack of truck data.

1.3 Literature Review

A brief literature review and comparison of them with this study yield following results:

Rossetter and Gerdes demonstrated how to aid the driver for lane keeping (by using superposed brake and steer interventions on the driver's inputs) using the potential fields and generalised damping functions [8]: The gradient of an arbitrarily chosen potential function (increasing when the deviation from the reference value increases) acts as a restoring force to aid the driver by the actuators (control input is determined by the gradient of the potential function) so that the vehicle is kept on the centre of the lane when the vehicle deviates from it. The arbitrary potential function could be chosen in a way that the gradient of it increases if the vehicle is approaching an obstacle on the road (intended for the collision avoidance manoeuvre). This paper resembles the thesis study to a great extent, with a slightly different approach on the control algorithm. However, it is more suitable for path control applications for passenger cars since the control algorithm proposed in the paper does not consider rollover problems and handling performance of heavy vehicles are restricted by low rollover thresholds especially on high μ surfaces.

Hiraoka, Nishihara and Kumamoto proposed a four wheel steering (4WS) control algorithm in order to better realise the path and path stability at the same time (due to the advantages of 4WS actuation) [9]. They defined centres of percussion for front and rear separately so as to be able to investigate the problem individually for two control points using sliding mode control. As could be understood, their study provides a different approach in vehicle path control by separating the front axle control from the rear axle control. The technique is promising (because it employs 4WS so that stability indicators of the vehicle are reported to reveal better values, e.g. lesser side slip angle) and is claimed to be robust with respect to system uncertainties. However, because the tag axle steering is decided not to be used in the thesis study from the beginning, it cannot be expected to extract fully relevant results from the aforementioned paper. Moreover, path planning, which is important to keep the heavy vehicle on the road without rolling it over, is not explained. Furthermore, the importance of speed reduction by braking is not mentioned in this study.

Thommyppillai, Evangelou and Sharp used an adaptive linear optimal time preview control so as to demonstrate car control at the absolute limits of handling [10]. They also compared the results with non-adaptive controls and showed the importance of adaptive controls which results from the reduction of the tyre lateral force generation

after adhesion limit has been exceeded (non-adaptive controls demand increased steering angles and therefore slip angles which results in limited utilisation of full adhesion). Their work in time preview control is somewhat similar to the "prediction distance" concept used in this thesis study, but not exactly matching it. They used a 3 degree-of-freedom planar model without load transfer; this approach may be acceptable for a race car as the centre of gravity of a race car is much lower than the CG of a heavy vehicle, however it is not acceptable for a study done on heavy vehicles! Moreover the paper states that the robustness is not important compared to the optimality of the controls "on the limits" and this is the opposite for an active safety system, especially considering the ultra-dynamic environment around the vehicle. In the thesis study, a simpler controller is integrated with a decision algorithm and thus the robustness is no longer a big problem to solve. Finally, the importance of speed reduction prior/during the manoeuvre is not mentioned in this paper, whereas this issue is pointed out in the thesis study.

Capability of an active safety system is usually limited by for instance, sensor systems that could be implemented onboard the vehicle or by the dynamics of the vehicle etc. It would be almost impossible or ultimately cumbersome and expensive to build only one system which could cope with all the hazardous situations in the traffic. As a result, it is important to understand the reason behind the accident with frequently observed kinematical data (e.g. speed range, dimensions of the obstacle in front etc.) in order to tune the system for this useful range. One way to understand the accidents and obtain useful kinematical range is to look at the accident databases.

2 Rear-end Target Scenarios from Accident Databases

In this study, ETAC (European Truck Accident Causation) database is used to obtain sufficient information about the predefined accident scenarios. It includes 624 accidents (in which at least one truck with a mass bigger than 3500 kg is involved) investigated between April 1st, 2004 and September 30th, 2006 in Germany, France, Italy, The Netherlands, Hungary, Slovenia and Spain. It is claimed to be representative [11].

Here, rear-end accident cases with its possible variants will be explained. When the rear-end cases are concerned, following variants could be listed:

- Rear-end collision due to slowing vehicle in front
- Rear-end collision due to vehicle in front moving slowly and at constant speed
- Rear-end collision due to a stopped vehicle in front

It has to be noted that the host vehicle in the following scenarios corresponds to the vehicle in which the intended active safety system is fitted and should intervene in the given target scenario; whereas the target vehicle corresponds to the one which is being hit by the host vehicle.

2.1 Rear-End Collisions Due to a Slowing Vehicle In Front

Brief Narrative

A truck (the host vehicle) is following the target vehicle (car, truck or bus) with a speed of V1, whereas the target vehicle is travelling with a speed of V2 (V1>V2). The target vehicle starts to decelerate and the host vehicle impacts it from the rear.

Range of V1 and V1-V2 (Relative Speed)

V1 is ranging from 47 km/h to 82 km/h. Median and average of the V1 data sample lie in between 50…60 km/h. Range of relative speed (V1-V2) is between 2 km/h and 20 km/h. Median and average of relative speed sample is approximately 15 km/h.

Road Details

Number of lanes (only for the direction of interest) for this scenario is found to be either 1 or 2. Single carriageways (one lane for each direction) are dominating.

2.2 Rear-End Collisions Due to a Vehicle In Front Moving Slowly and At Constant Speed

Brief Narrative

A truck (the host vehicle) is following the target vehicle (car, truck or bus) with a speed of V1, whereas the target vehicle is travelling with a speed of V2 (V1>V2). The host vehicle continues to move towards the target vehicle travelling at constant speed and hits it from its rear.

Range of V1 and V1-V2 (Relative Speed)

V1 is ranging from 60 km/h to 102 km/h. The median of V1 data sample is 90 km/h. In about 78% of all cases, V1 is between 80 km/h and 102 km/h. Range of relative speed (V1-V2) is between 10 km/h and 60 km/h. The median of this sample is 25 km/h. In 78% of all cases, relative speed is between 10 km/h and 40 km/h.

Road Details

Number of lanes (for the direction of interest) for this scenario is found to be either 2 or 3. Dual carriageways (2-lanes in each direction) are dominating.

2.3 Rear-End Collisions Due to a Stopped Vehicle In Front

Brief Narrative

A truck (the host vehicle) is approaching the target vehicle (car, truck or bus) with a speed of V1. The target vehicle is stopped. Driver of the host vehicle recognises the target vehicle very late, he brakes before the crash but the deceleration is not enough to avoid the accident.

Speed Range for V1

It is ranging from 12 km/h to 90 km/h. The median of the sample is 67 km/h. In more than 47% of the cases, speeds are between 70 km/h and 90 km/h.

Road Details

Number of lanes (only for the direction of interest) for this scenario can be one, two, three or four. In about 79% of the cases, the number of lanes is less than three.

The number of variants could be extended even further! In this study, the accident type which is “Rear-end collisions due to a stopped vehicle in front” is chosen as the problem to focus on since it is easy to understand and therefore easier to come up with a solution.

3 Modelling of a Heavy Truck

It is known from engineering observations and real-life experience that a truck is usually subject to rollover before losing its directional stability in evasive manoeuvres. This statement is correct when the maximum adhesion coefficient between the tyre and the ground is high enough. The question of "how high", of course, depends on the vehicle suspension parameters and CG height; but roughly one can say that a severe manoeuvre performed on a surface with a maximum adhesion coefficient of $\mu = 0.4 - 0.6$ may be enough for rollover unless the truck is equipped with a special countermeasure, e.g. ESP. As a result, apart from the need for a nonlinear two-track model particularly suitable for evasive manoeuvres and differential brake interventions, a good-enough roll and load transfer model should be built.

In this work, a nonlinear four degree of freedom model (longitudinal, lateral, yaw and body roll) is developed.

3.1 Axle and Wheel Notations

The notation system for the axles and wheels are depicted in Figure 3:

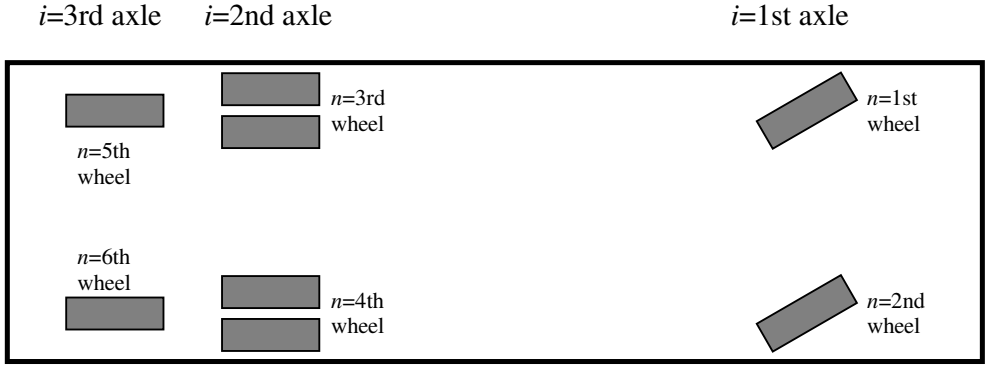

Figure 3 A simple sketch showing the notations of the axles and wheels.

3.2 Tyre Model and Relevant Assumptions

A nonlinear tyre model will be required if a severe collision avoidance manoeuvre is studied and simulated. The problem here is that exact tyre data, except the cornering stiffness with respect to the normal load on the tyre, was not available. Therefore, some engineering approximations based on previous experience from the investigation of a typical tyre lateral force versus slip angle characteristic had to be made. Particular attention was paid to obtain reasonable values.

3.2.1 Adhesion Coefficient and Its Alteration with the Vertical Load

The maximum adhesion coefficient decreases with the increasing vertical load for a pneumatic tyre. A truck tyre, compared to a passenger car tyre, is more sensitive to increased vertical load when adhesion coefficient is concerned [12]. Figure 4 depicts this phenomenon clearly:

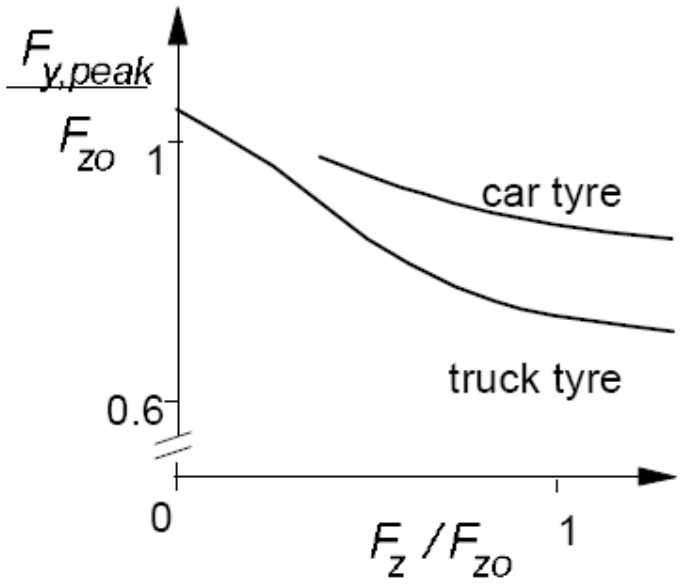

Figure 4 *A comparison of a truck tyre and a passenger car tyre for maximum adhesion coefficients at different normal loads. F_{z0} is the rated load (Adopted from Ref. [12]).*

As can be seen from the Figure 4, the relation between the vertical load and the maximum adhesion coefficient is nonlinear. However, in order to simplify the approximation process, a linear relation is assumed. It is given (for the i-th axle and n-th wheel) in Equation 1.

$$\mu_n = -\mu_{1,i} F_{z,n} + \mu_{2,i} \tag{1}$$

Based on the values given in Table 1.3 of [13], it is assumed that the maximum adhesion coefficient at laden static load is 0.8 for all axles. It is further assumed that this value drops down to 0.75 in the presence of extreme load transfer, i.e. when the inner wheel is lifted up due to a severe manoeuvre.

To be able to set $\mu_{1,i}$ and $\mu_{2,i}$ for the tyres on different axles, the laden static load distribution must be known. For a three axle truck, it is known that the maximum permissible total mass of the vehicle according to EU regulations is 26 tonnes, with the assumption of using air suspension [14]. From Volvo's technical sheet [15], it could be seen that the nominal load of a tandem axle of a sample 6x2 truck, with the traction torque applied on the second axle, is 19 tonnes. Load distribution between the second and the third axles are not the same; the second axle has a capacity of carrying

11.5 tonnes and the third (tag) axle has a capacity of carrying 7.5 tonnes. The traction axle is allowed to have a maximum load of 11.5 tonnes again according to [14], hence this load distribution already complies with the road regulations in Europe. Recalling the rule that the total mass of a three axle truck may not exceed 26 tonnes, one may conclude that a fully laden three axle truck (of course, complying with the road regulations) has 7 tonnes on the first (front) axle. To sum up; first, second and third axle loads are assumed to be 7, 11.5 and 7.5 tonnes, respectively.

Assuming that the CG is located on the mid-plane of the truck, following relations could be written for the maximum adhesion coefficients per tyre:

First axle (μ_1 and μ_2):

$$\mu_{1,1} = \frac{0.1}{7000 \cdot 9.81} \ [\mathrm{N^{-1}}]$$

$$\mu_{2,1} = 0.85 \ [-]$$

Second axle (μ_3 and μ_4):

$$\mu_{1,2} = \frac{0.1}{5750 \cdot 9.81} [\mathrm{N^{-1}}]$$

$$\mu_{2,2} = 0.85 \ [-]$$

Note that the 6x2 truck is equipped with dual tyres on the second axle. The coefficients given above are given for one single tyre. In the presence of load transfer and in static conditions, each individual tyre in the dual tyre combination is assumed to carry equal amount of vertical load.

Third axle (μ_5 and μ_6):

$$\mu_{1,3} = \frac{0.1}{7500 \cdot 9.81} [\mathrm{N^{-1}}]$$

$$\mu_{2,3} = 0.85 \ [-]$$

3.2.2 Cornering Stiffness and Its Alteration with the Vertical Load

The cornering stiffness, $\left(\frac{\partial F_y}{\partial \alpha}\right)_{\alpha=0}$, increases degressively (i.e. the second derivative of cornering stiffness with respect to the normal load is negative) with the increasing vertical load for a pneumatic tyre. One recommendation to express this is to use a quadratic function. This function looks like as follows (for the i-th axle, n-th wheel):

$$C_{\alpha,n} = C_{1,i}\left(F_{z,n}\right)^2 + C_{2,i}\left(F_{z,n}\right) \qquad (2)$$

The coefficients are provided by Volvo 3P and they are given as follows:

First axle ($C_{\alpha,1}$ and $C_{\alpha,2}$):

$C_{1,1} = -2.10^{-5}$ [N^{-1}.rad^{-1}]

$C_{2,1} = 5.8614$ [rad^{-1}]

Second and third axles ($C_{\alpha3}$, $C_{\alpha4}$, $C_{\alpha5}$ and $C_{\alpha6}$):

$C_{1,2} = C_{1,3} = -2.10^{-5}$ [N^{-1}.rad^{-1}]

$C_{2,2} = C_{2,3} = 6.515$ [rad^{-1}]

Note that the comment made about the dual tyres in the maximum adhesion coefficient calculation is also valid here.

3.2.3 Estimation of the Magic Formula Parameters and Transient Force Generation

The Magic Tyre Formula is a very useful tool to model tyre forces with respect to the longitudinal slip/slip angle. It provides a "magically" good fit to the experimental tyre data, thus making it attractive to use in vehicle dynamics simulations. The mathematical expression for it is given in the following (assuming zero camber, conicity and ply-steer):

$$F_{y,mf,n} = D_n \sin\{C_n \arctan[B_n\alpha_n - E_n(B_n\alpha_n - \arctan(B_n\alpha_n))]\} \quad (3)$$

Note that since the longitudinal slip is not considered in the simulation, lateral tyre force versus slip angle characteristics are used in this work; hence the formulation expressing only the tyre lateral characteristics is given in Equation 3.

The coefficients *D*, *C*, *B* and *E* can be determined by trial and error method (or using regression techniques) if the experimental tyre force versus slip angle characteristic is known. The definition of the coefficients are summarised in Table 1. The reader is encouraged to refer to [12] for further information about this.

Table 1 Definitions of the Magic Tyre Formula parameters

Coefficient	Definition
D	Peak value
C	Shape factor
E	Curvature factor
B	Stiffness factor

The peak value (D_n) can simply be calculated as follows:

$$D_n = \mu_n F_{z,n} \tag{4}$$

Shape and curvature factors (C_n and E_n) can be calculated by using the Equations 5 and 6 given in Reference [12]:

$$C_n = 1 \pm \left(1 - \frac{2}{\pi} \arcsin\left(\frac{F_{y,a,n}}{D_n} \right) \right) \tag{5}$$

$$E_n = \frac{B_n \alpha_{m,n} - \tan\left(\frac{\pi}{2C_n} \right)}{B_n \alpha_{m,n} - \arctan\left(B_n \alpha_{m,n} \right)} \quad (\text{for } C_n > 1) \tag{6}$$

$F_{y,a,n}$ and $\alpha_{m,n}$ are the lateral force vs. slip angle characteristic's horizontal asymptote and the slip angle where the maximum lateral force is generated, respectively. Based on Table 1.3 of [13], the assumption of the ratio ($F_{y,a,n}/D_n$=0.75) seems reasonable for a dry and hard surface. The slip angle where the maximum lateral force is generated (α_m) changes with the vertical load (it increases with the increasing vertical load for pneumatic tyres). The following figure is an evidence for this statement:

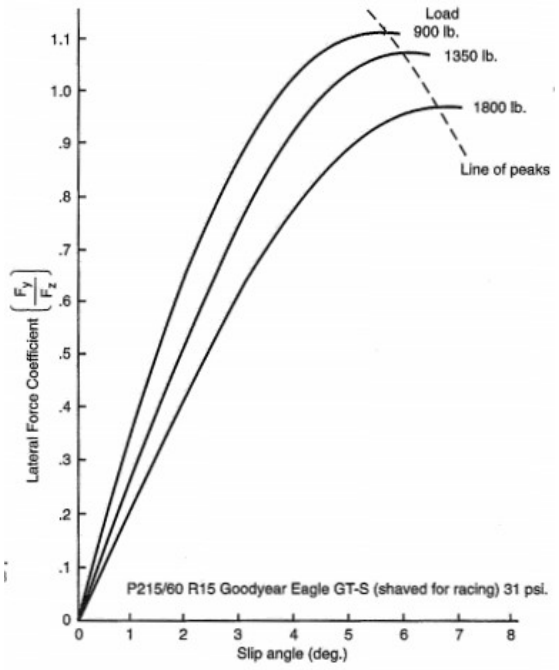

Figure 5 *The tyre side force vs. slip angle characteristic for a pneumatic tyre revealing how the peak shifts with increasing vertical load (Adopted from Ref. [17]).*

A linear function is assumed for this change (lateral shift of peak tyre force point) and the mathematical expressions used to determine $\alpha_{m,n}$ is given as follows (the coefficients are adjusted so that the $\alpha_{m,n} = 10°$ in the vicinity of zero vertical load and $\alpha_{m,n} = 15°$ when the inner wheel is lifted up):

For the first axle ($\alpha_{m,1}$ and $\alpha_{m,2}$):

$$\alpha_{m,n} = \left(10 + \frac{5}{7000 \cdot 9.81} F_{z,n}\right) \frac{\pi}{180} \quad \text{[rad]} \tag{7}$$

For the second axle ($\alpha_{m,3}$ and $\alpha_{m,4}$):

$$\alpha_{m,n} = \left(10 + \frac{5}{5750 \cdot 9.81} F_{z,n}\right) \frac{\pi}{180} \quad \text{[rad]} \tag{8}$$

Note that the comment made about the dual wheels in the maximum adhesion coefficient calculation is also valid here.

For the third axle ($\alpha_{m,5}$ and $\alpha_{m,6}$):

$$\alpha_{m,n} = \left(10 + \frac{5}{7500 \cdot 9.81} F_{z,n}\right) \frac{\pi}{180} \quad \text{[rad]} \tag{9}$$

As the necessary information to calculate C_n and D_n and $C_{\alpha,n}$ are provided, B_n can be computed:

$$B_n = \frac{B_n C_n D_n}{C_n D_n} = \frac{C_{\alpha,n}}{C_n D_n} \tag{10}$$

When a tyre generates both a longitudinal and a lateral force, then any of them has to be less than the adhesion limit. None of them will be equal to the adhesion limit (=D_n) if this is the case. This phenomenon can be demonstrated by Kamm's circle, also known as the friction circle. This is a circle with a constant radius equal to the adhesion limit. The resultant force of the generated longitudinal and lateral force cannot exceed the circle's border. In order to take this into account, the limit side force which is denoted by "D_n" in Magic Tyre Formula is replaced by the following expression:

$$D_n \rightarrow \sqrt{D_n^2 - F_{x,n}^2} = \sqrt{\left(\mu_n F_{z,n}\right)^2 - F_{x,n}^2} \tag{11}$$

As can be seen in the Equation 11, a negative vertical force (usually encountered in the simulations when one wheel is lifted up due to severe cornering) will also yield a positive D_n, which will result in a lateral tyre force. Extensive attention has to be paid on this unless roll degree of freedom of the axle is modelled in a vehicle dynamics simulation. Simulation has to be aborted when this is the case and one wheel load turns out to be negative.

Not only the lateral force, but also the longitudinal force has to be limited. When the wheel is locked due to intense braking, the whole wheel starts to slide and the force generation is altered. The wheel now acts like a solid object exposed to Coulomb friction and sliding on the road surface. This means that the resultant tyre force is parallel but in opposite direction to the sliding velocity vector at the tyre contact patch. When an excessive traction torque is applied on the wheel, the force generation is not altered because a wheel on which a traction torque is applied cannot behave like a locked wheel (i.e. absolute value of the longitudinal slip never reaches 100% unless the vehicle is fixed). Using this knowledge, following interval can be written for the traction force:

$$-\mu_n F_{z,n} \cos\alpha_n \leq F_{x,n} \leq \mu_n F_{z,n} \tag{12}$$

One important point here is the dependence of adhesion coefficient on the slip angle for big slip angles. Once the peak point in the tyre lateral force vs. slip angle characteristic is exceeded, the whole tread starts to slide. After this point, the more the slip angle is increased the less the adhesion coefficient becomes. This could be explained by using a Stribeck diagram [29], however the explanation is not going to be given here. When full sliding starts, then the available adhesion coefficient which will also be used to calculate the radius of the friction circle is assumed to be as follows (calculation is performed for zero longitudinal force):

$$\mu_n = \frac{\left|F_{y,mf,n}\right|}{F_{z,n}}, \text{ when } |\alpha_n| > \alpha_{m,n} \tag{13}$$

The force calculated from the Magic Tyre Formula is the steady state lateral force. However, it is known that in practice, a tyre must translate in order to generate a certain amount of slip angle (generation of slip angle = generation of side force). This means that the side force build-up is not instantaneous since some time and translation distance is needed to stretch the tyre components. The required distance which is needed for the tyre to generate 63.2% of a step change in steady-state lateral force (here, this is calculated by using the Magic Formula) is defined as "relaxation length" (σ). The first order approximation for the build-up of the tyre lateral force is given as follows ($v_{x,n}$ is the longitudinal speed at the contact patch of each wheel):

$$\frac{\sigma_{y,n}}{v_{x,n}}\dot{F}_{y,n} + F_{y,n} = F_{y,mf,n} \tag{14}$$

Note that the differential equation above is not a linear one since $v_{x,n}$ is not constant. From References [18] and [19], lateral tyre relaxation lengths for all tyres are assumed to be $\sigma_{y,n} = 0.4$ m.

The same concept also applies for the longitudinal force build-up. One can write the following expression to express the gradual first order increase/decrease of the longitudinal forces. The input to the differential equation in this study is the brake forces applied by the path following controller (note that the rim force, $F_{x,rim,n}$, is a fictitious internal force acting on the rim that results in the same tyre force in steady state):

$$\frac{\sigma_{x,n}}{v_{x,n}}\dot{F}_{x,n} + F_{x,n} = F_{x,rim,n} \tag{15}$$

From a literature survey, one could find that the longitudinal relaxation length is roughly the half of the lateral relaxation. This could be deduced from the sample numerical values provided in [16] and [19]. Hence, the longitudinal relaxation length is assumed to be $\sigma_{x,n} = 0.2$ m for all tyres.

3.3 Vehicle Model and Relevant Assumptions

Because this study involves path control and stability in severe collision avoidance manoeuvres, a more realistic vehicle model is needed. Simple linear bicycle models provide acceptable results as long as the lateral accelerations and yaw rates remain very low during the manoeuvre, thus they are not suitable for this application. However, one should keep in mind that so as to obtain realistic results from a realistic simulation, the input data has to be as accurate as possible. In this work, it is assumed that the assumed and acquired truck chassis data represent a physical truck with enough accuracy.

3.3.1 Planar Free Body Diagram of the Truck

A schematic plan view of the truck together with the most important tyre forces, steering angles and coordinate system are given in Figure 6:

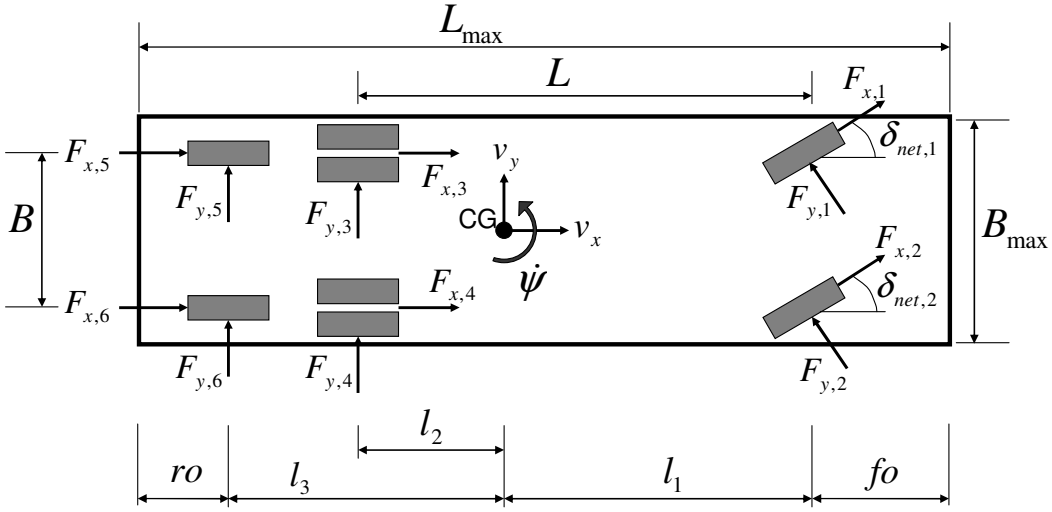

Figure 6 *Schematic planar sketch of the 6x2 truck. Note that only the front axle is steered; the subscript "net" indicates the net steering angle after the elastokinematical effects and the steering compliance. The 2nd and the 3rd axles are not steered; however due to the elastokinematics, the wheels on these axles are deflected by small steering angles ($\delta_{net,3}$, $\delta_{net,4}$ and so on) which are not shown in the sketch. The gross dimensions L_{max} and B_{max} are particularly important for collision avoidance manoeuvres.*

3.3.2 Planar Equations of Motion for the Truck

The planar equations of motion for the 4 degree-of-freedom model written in ISO coordinate system are given as follows:

$$m = m_{unspr} + m_{spr} \tag{16}$$

Longitudinal (x) equation (recall that pitch dynamics and cross terms due to yaw, roll and their time derivatives are neglected):

$$\Sigma F_x = ma_x = m\left(\dot{v}_x - v_y\dot{\psi}\right) \tag{17}$$

$$m\left(\dot{v}_x - v_y\dot{\psi}\right) = F_{x,1}\cos\delta_{net,1} - F_{y,1}\sin\delta_{net,1} + F_{x,2}\cos\delta_{net,2} - F_{y,2}\sin\delta_{net,2} + F_{x,3}\cos\delta_{net,3} - F_{y,3}\sin\delta_{net,3} + F_{x,4}\cos\delta_{net,4} - F_{y,4}\sin\delta_{net,4} + F_{x,5}\cos\delta_{net,5} - F_{y,5}\sin\delta_{net,5} + F_{x,6}\cos\delta_{net,6} - F_{y,6}\sin\delta_{net,6} \quad (18)$$

Lateral (y) equation (cross terms are still being neglected):

$$\Sigma F_y = ma_y = m\left(\dot{v}_y + v_x\dot{\psi}\right) - m_{spr}\ddot{\phi}h' \quad (19)$$

$$m\left(\dot{v}_y + v_x\dot{\psi}\right) - m_{spr}\ddot{\phi}h' = F_{y,1}\cos\delta_{net,1} + F_{x,1}\sin\delta_{net,1} + F_{y,2}\cos\delta_{net,2} + F_{x,2}\sin\delta_{net,2} + F_{y,3}\cos\delta_{net,3} + F_{x,3}\sin\delta_{net,3} + F_{y,4}\cos\delta_{net,4} + F_{x,4}\sin\delta_{net,4} + F_{y,5}\cos\delta_{net,5} + F_{x,5}\sin\delta_{net,5} + F_{y,6}\cos\delta_{net,6} + F_{x,6}\sin\delta_{net,6} \quad (20)$$

Moment (z) equation:

$$\Sigma M_z = I_{zz}\ddot{\psi} \quad (21)$$

$$I_{zz}\ddot{\psi} = \left(F_{x,1}\sin\delta_{net,1} + F_{y,1}\cos\delta_{net,1}\right)l_1 - \left(F_{x,1}\cos\delta_{net,1} - F_{y,1}\sin\delta_{net,1}\right)\frac{B}{2} + \left(F_{x,2}\sin\delta_{net,2} + F_{y,2}\cos\delta_{net,2}\right)l_1 + \left(F_{x,2}\cos\delta_{net,2} - F_{y,2}\sin\delta_{net,2}\right)\frac{B}{2} - \left(F_{x,3}\sin\delta_{net,3} + F_{y,3}\cos\delta_{net,3}\right)l_2 - \left(F_{x,3}\cos\delta_{net,3} - F_{y,3}\sin\delta_{net,3}\right)\frac{B}{2} - \left(F_{x,4}\sin\delta_{net,4} + F_{y,4}\cos\delta_{net,4}\right)l_2 + \left(F_{x,4}\cos\delta_{net,4} - F_{y,4}\sin\delta_{net,4}\right)\frac{B}{2} - \left(F_{x,5}\sin\delta_{net,5} + F_{y,5}\cos\delta_{net,5}\right)l_3 - \left(F_{x,5}\cos\delta_{net,5} - F_{y,5}\sin\delta_{net,5}\right)\frac{B}{2} - \left(F_{x,6}\sin\delta_{net,6} + F_{y,6}\cos\delta_{net,6}\right)l_3 + \left(F_{x,6}\cos\delta_{net,6} - F_{y,6}\sin\delta_{net,6}\right)\frac{B}{2} \quad (22)$$

3.3.3 Roll of Sprung Mass

As can be seen from the lateral (y) equation of motion (Equation 19), an additional term appears due to the roll acceleration of the sprung mass. Because there is a distance between centre of gravity and the roll centre of sprung mass, roll acceleration induces an additional linear acceleration which has to be taken into account while setting up the lateral (y) equation. Roll acceleration is calculated from differential equation expressing the roll dynamics of the sprung mass. By observing Figure 7, the differential equation can be derived.

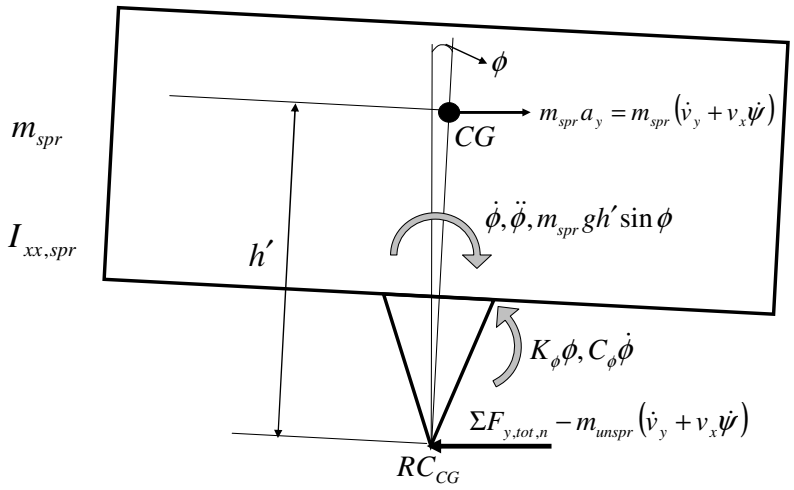

Figure 7 *Free body diagram of the sprung mass. Note that the static equilibrium condition is taken as the reference; hence the vertical forces that balance each other are not shown. The location of the centre of gravity for the sprung mass is assumed to be the same as the location of the centre of gravity for the whole vehicle since $m_{spr}/m = 0.9 \approx 1$.*

Summing the moments about the RC_{CG}, using the parallel axis theorem (Steiner theorem) and assuming small angles (roll angles do not exceed 10°):

$$\Sigma M_{RC_{CG}} = \left(I_{xx,spr} + m_{spr}h'^2\right)\ddot{\phi} \tag{23}$$

$$\left(I_{xx,spr} + m_{spr}h'^2\right)\ddot{\phi} = -K_\phi\phi - C_\phi\dot{\phi} + m_{spr}gh'\phi + m_{spr}h'\left(\dot{v}_y + v_x\dot{\psi}\right) \tag{24}$$

3.3.4 Lateral and Longitudinal Load Transfers

By using Equation 24, transient lateral load transfer can be calculated. In order to do this, free body diagram of the axles should be drawn and observed. Free body diagram of *i*-th axle is given in Figure 8. Assuming that none of the wheels is lifted, the load transfer on *i*-th axle could be determined.

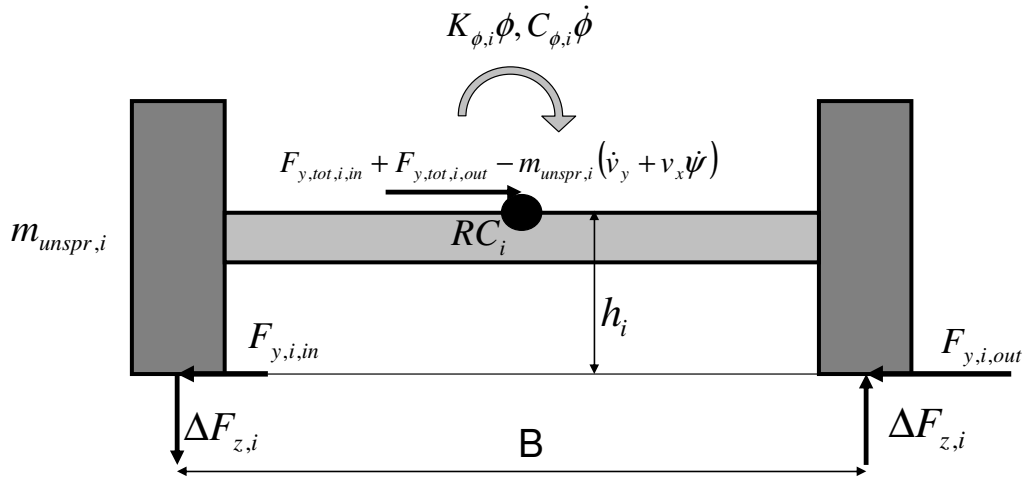

Figure 8 *Free body diagram of the i-th axle. Note that the static equilibrium condition is taken as the reference; hence the vertical forces that balance each other are not shown. The subscript "tot" is used since a longitudinal force applied on a steered wheel has a component on lateral direction and this has to be taken into account in calculating the amount of load transfer. None of the longitudinal forces is shown on the figure.*

Summing moments around RC_i yields:

$$\Delta F_{z,i} = \frac{C_{\phi,i}\dot{\phi} + K_{\phi,i}\phi + \left(F_{y,tot,i,in} + F_{y,tot,i,out}\right)h_i}{B} \tag{25}$$

Note that additional effect of the acceleration term $\dot{\phi}^2 h'$ on vertical forces is neglected.

In order to be able to calculate the load transfer on tandem axles, some assumptions and definitions must be made. Tandem axles are designed in a way that it prevents one axle from being overloaded and especially causing damage to the road when negotiating uneven surfaces [20]. One simple way to realise this is to use scale-beam principle [7] where the two axles are connected to one big leaf spring and the leaf spring is mounted on the chassis in a way that it can pivot and prevent any of the axle connected on this group to lose contact with the road. The basic construction of it can be seen in Figure 9:

Figure 9 *A tandem axle construction by Mercedes (Adopted from Ref. [21]). The axle group is able to pivot with the help of rotating joint where the brand badge is located.*

On the truck of interest, this type of system is assumed. However, since the axles on the tandem axle group of the truck of interest carry different loads (2nd axle carries 11.5 tonnes and 3rd axle carries 7.5 tonnes), the pivot point should be located close to the second axle instead of in the middle of the second and the third axles to keep the static equilibrium. According to the Volvo technical sheet [15], the distance from this pivot point (or the virtual load centre of the tandem axle) to the first axle is called the theoretical wheelbase (L_t). By using this theoretical wheelbase definition, the three-axle vehicle can be reduced to a two-axle one whose axle loads are 7 tonnes and 19 tonnes, respectively.

The theoretical wheelbase could be calculated as follows:

$$L_t = L + \frac{F_{z,i=,stat}}{F_{z,i=2,stat} + F_{z,i=3,stat}} \left(l_3 - l_2 \right) \tag{26}$$

Note that the distance ($l_3 - l_2$) is also called bogie spread (BS) as this type of tandem axle is also known as bogie axle. Substituting the numerical values (these values are taken from Ref. [15]) into the equation above results:

$$L_t = 4.900 + \frac{7.5}{11.5 + 7.5} 1.370 = 5.441 \text{ m}$$

The value calculated above is exactly what is given for this type of truck in the technical sheet. It is important to distinguish the difference between the theoretical wheelbase and the equivalent wheelbase whose definition is usually seen in vehicle dynamics texts. A three-axle vehicle will have the similar steady-state linear handling properties if compared with a two-axle vehicle having the equivalent front tyres, rear tyres and equivalent wheelbase [22]. The equivalent wheelbase is always bigger than $L+(BS/2)$ value, whereas in the truck of interest the theoretical wheelbase, which is the "load centre" on the tandem axle, is less than the value mentioned. The theoretical wheelbase definition will become useful when calculating the centre of gravity position and load transfers.

The centre of gravity position on "x" axis could be determined by calculating the distance l_1:

$$l_1 = \frac{F_{z,i=2,stat} + F_{z,i=3,stat}}{\Sigma F_{z,i,stat}} L_t \tag{27}$$

Substituting numerical values into Equation 27 (The numerical value is given to the reader here to make him/her have a "feeling" about the CG location of a laden truck):

$$l_1 = \frac{11.5 + 7.5}{7 + 11.5 + 7.5} 5.441 = 3.976 \text{ m}$$

l_2 and l_3 now become straightforward to calculate:

$$l_2 = L - l_1 \tag{28}$$

$$l_3 = L + BS - l_1 \tag{29}$$

Substituting the numerical values into Equations 28 and 29:

$$l_2 = 4.900 - 3.976 = 0.924 \text{ m}$$

$$l_3 = 4.900 + 1.37 - 3.976 = 2.294 \text{ m}$$

The longitudinal load transfer can now be calculated by assuming that the truck is a two-axle vehicle with the axle loads of 7 tonnes and 19 tonnes and spacing between these axles are equal to the theoretical wheelbase. Once the total longitudinal load transfer on the tandem axle is calculated, the longitudinal load transfer on the second and on the third axles could be determined by using the moment equilibrium, i.e. they are proportional to the static loads on the axles mentioned (This statement could easily be proven by observing the ratio between the lever arm distances to the pivot point). The mathematical expressions are given as follows:

$$\Delta F_{z,n=1,2} = -ma_x \frac{h}{2L_t} \tag{30}$$

$$\Delta F_{z,i=2+3} = ma_x \frac{h}{L_t} \tag{31}$$

and;

$$\Delta F_{z,n=3,4} = ma_x \frac{h}{4L_t} \left(\frac{F_{z,i=2,stat}}{F_{z,i=2,stat} + F_{z,i=3,stat}} \right) \tag{32}$$

$$\Delta F_{z,n=5,6} = ma_x \frac{h}{2L_t} \left(\frac{F_{z,i=3,stat}}{F_{z,i=2,stat} + F_{z,i=3,stat}} \right) \tag{33}$$

Note that the amount of longitudinal load transfer is given per tyre! In the vehicle data, the centre of gravity position is not directly given. Instead, roll centre height at each axle and the height of CG above the roll axis are provided. Here, it is assumed that the (assumed) pivot point absorbs all the lateral forces from the tyres on the second and the third axles, thus the roll centre height for the tandem axle group becomes the same as the height of the (assumed) pivot point. In a typical 3-axle Volvo truck, roll centre heights at the 2nd and the 3rd axles are usually equal ($h_2 = h_3$) and therefore RC height for the tandem group is equal to one of them or the average of them ($h_{tandem} = h_2 = h_3 = (h_2 + h_3)/2$). Consequently, the CG height could be calculated in Equation 34:

$$h = h_1 + \left(\frac{h_2 + h_3}{2} - h_1 \right) \frac{l_1}{L_t} + h' \tag{34}$$

Using the same assumptions that are utilised to calculate the longitudinal load transfer and the CG height, lateral load transfer could be calculated. For the front axle, lateral load transfer can easily be calculated by utilising Equation 25. For the second and the third axles, it is assumed that the total amount of load transfer on the tandem is shared between them equally since roll stiffness and roll damping coefficients for the second and the third axles are given to be the same ($K_{\phi,1} = K_{\phi,2}$ and $C_{\phi,1} = C_{\phi,2}$). The lateral load transfer expression for them is given in Equation 35:

$$\Delta F_{z,i=2,3} = \frac{1}{2} \left(\frac{\left(C_{\phi,2} + C_{\phi,3}\right)\dot{\phi} + \left(K_{\phi,2} + K_{\phi,3}\right)\phi + \left(F_{y,tot,i=2+3,in} + F_{y,tot,i=2+3,out}\right)h_{i=2,3}}{B} \right) \tag{35}$$

3.3.5 Slip and Net Steering Angles

The calculation of tyre forces does require the determination of individual slip angles at each tyre. In a two track vehicle model, trackwidth and yaw rate induce an additional effect on the longitudinal speed of the tyre contact patch and this has to be taken into account unlike what is done in a single track (bicycle) model. The slip angles on each wheel can be calculated by the generic formula given below:

$$\alpha_n = \delta_{net,n} - \arctan\left(\frac{v_{y,n}}{|v_{x,n}|} \right) \tag{36}$$

The absolute value of the longitudinal speed at each wheel has to be taken since the direction of the tyre force is only determined by the direction of the lateral speed (regardless of the direction of the longitudinal speed) at each contact patch. For each wheel, using Equation 36, the slip angles could be written as follows (Note that the same slip angles are assumed for the tyres on the dual wheel combination [second axle]):

$$\alpha_1 = \delta_{net,1} - \arctan\left(\frac{v_y + l_1\dot{\psi}}{\left|v_x - \frac{B}{2}\dot{\psi}\right|}\right) \tag{37}$$

$$\alpha_2 = \delta_{net,2} - \arctan\left(\frac{v_y + l_1\dot{\psi}}{\left|v_x + \frac{B}{2}\dot{\psi}\right|}\right) \tag{38}$$

$$\alpha_3 = \delta_{net,3} - \arctan\left(\frac{v_y - l_2\dot{\psi}}{\left|v_x - \frac{B}{2}\dot{\psi}\right|}\right) \tag{39}$$

$$\alpha_4 = \delta_{net,4} - \arctan\left(\frac{v_y - l_2\dot{\psi}}{\left|v_x + \frac{B}{2}\dot{\psi}\right|}\right) \tag{40}$$

$$\alpha_5 = \delta_{net,5} - \arctan\left(\frac{v_y - l_3\dot{\psi}}{\left|v_x - \frac{B}{2}\dot{\psi}\right|}\right) \tag{41}$$

$$\alpha_6 = \delta_{net,6} - \arctan\left(\frac{v_y - l_3\dot{\psi}}{\left|v_x + \frac{B}{2}\dot{\psi}\right|}\right) \tag{42}$$

In this study, only the front axle is assumed to be steerable. However, this does not mean that the steering angle for the wheels on the second and the third axles is zero. Due to the kinematics and elasticity of the axle/suspension system, wheels/axles deflect in the presence of the lateral forces, longitudinal forces, re-aligning moments and sprung mass roll. The "net steering angles" on all axles are determined after taking the kinematic/elastokinematic effects into consideration. Three main effects

can be listed here: Roll steer, lateral force steer and aligning moment steer. Usually; roll steer, which is caused by one side of the axle moving forward and the other side of the axle moving backward due to the asymmetric deflection of the leaf springs and/or the geometric location as well as the kinematics of the suspension links (including the steering links), is the dominant effect for the trucks compared to the other two. In this study, only the roll steer is considered because of its dominance over the other effects and the lack of truck data. Roll steer is normally a nonlinear function of the roll angle, but due to small roll angles and again lack of truck data, it is assumed to be a linear function of the roll angle. A roughly estimated roll steer coefficients have been acquired from the References [17] and [23] for the first (towards understeer), for the second (towards oversteer) and for the third axles (towards oversteer). In general, when the suspension is concerned, the wheel deflections towards toe-in are assigned to be positive (hence the roll steer coefficient is positive if the wheel deflection is towards toe-in for a positive roll angle). The reader of the thesis should be aware that this sign convention is used while expressing the net steer angles. They are given as follows:

$$\delta_{net,1} = \delta_1 - \varepsilon_1 \phi \tag{43}$$

$$\delta_{net,2} = \delta_2 + \varepsilon_2 \phi \tag{44}$$

$$\delta_{net,3} = -\varepsilon_3 \phi \tag{45}$$

$$\delta_{net,4} = \varepsilon_4 \phi \tag{46}$$

$$\delta_{net,5} = -\varepsilon_5 \phi \tag{47}$$

$$\delta_{net,6} = \varepsilon_6 \phi \tag{48}$$

The commanded steering wheel input is transmitted to the wheels via a recirculating ball steering gearbox and corresponding steering links. The ratio between the steering wheel angle and the road wheel angle is not constant! However, due to lack of truck data, the steering ratio is assumed to be constant and $i_s = 20$. There are some losses while transmitting the steering wheel motion into the road wheel motion due to the elasticity on the whole steering system (including the steering column). When the tyres generate side forces, these forces "compress" the whole system, thus leading to a reduction in steer angle. The constitutive relation for this is again nonlinear, but a linear relation is assumed. The lumped compliance for the system is taken from the Reference [17]. The expression for the "reduced" (but not the net!) road wheel angles are given as follows:

$$\delta_1 = \delta_2 = \frac{\delta_{SWA}}{i_s} - c_\delta \left(F_{y,1} + F_{y,2} \right) \tag{49}$$

4 Path Control Strategies

4.1 Path Control Problem

The path control for this study could be defined as how to keep the truck on the path which can be one possible definition of a severe path for a double lane change manoeuvre. The truck follows a sinusoidal function from changing one lane to another, where the spatial frequency and the amplitude of it define how much a truck has to move laterally in a given longitudinal distance in order to avoid the obstacle. The same sinusoidal function is utilised to realise the second lane change manoeuvre, but the truck needs to travel straight for a certain longitudinal distance.

As explained before, the targeted accident scenario which the active safety system could handle is "rear-end collisions due to stopped vehicle in front". Hence, a double lane change manoeuvre could be used to test the strategy. The manoeuvre proposed here resembles an ISO double lane change manoeuvre (initial speed in this manoeuvre is 80 km/h), however it employs different geometric data to test the limits of the vehicle and the control algorithm. It is given in Figure 10:

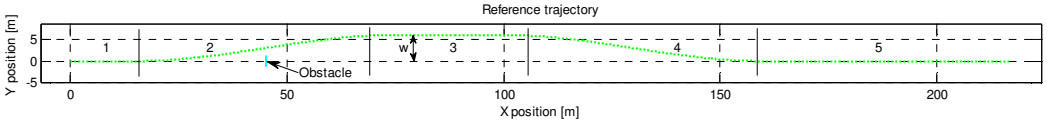

Figure 10 The sample double lane change path. Note that axes use the same scale.

A brief explanation about the regions 1 to 5 is given in the following:

1: Initial straight section (15 m)

2: Sinusoidal lane change ("w" metre of lateral displacement in 60 m)

3: Intermediate straight section (25 m)

4: Sinusoidal lane change ("w" metre of lateral displacement in 60 m)

5: Final straight section

The reason why sinusoidal functions are preferred instead of a clothoid (which provides a smooth and continuous radius of curvature) is that sinusoidal functions are easy to handle if the distance (e.g. 60 m) to get a particular lateral displacement and that particular lateral displacement (e.g. "w") have to be changed for tests.

Note that the width of the obstacle is defined as 2.6 m. According to the road regulations, the total width of the vehicle should not exceed 2.55 m unless a special permission is given. This value is rounded to 2.6 m and this is the reason why the obstacle width is assigned to be 2.6 m. It is assumed that the right edges of the obstacle (i.e. the stopped vehicle in front) and the truck are aligned. This assumption

necessitates the escape path to be even more severe compared to the case where the midplanes of the obstacle and the truck are aligned.

4.2 General Information about Actuators

Here, no brake delays are modelled due to lack of truck data. In a brake system, the time required for the brake pads to grip the brake drum/brake disc can be defined as "brake delay" or "brake slack". According to the Reference [24], this time is about 0.04 s which is rather long since it corresponds to 1.11 m of longitudinal distance when panic-braking at 100 km/h. However, the brake slack could easily be minimised with today's technology. When the onboard sensor systems detect an imminent danger in front of the vehicle, the corresponding active safety system can "pre-charge" the brake system (and reversibility of this action makes it suitable to be used in all critical situations) and reduce the brake slack significantly prior to a panic-braking.

It is assumed that brake system behaves as a first order linear system with a time constant of $\tau_{brake} = 0.1$ s. The equation expressing this could be given as follows (note that the control force is a fictitious force that results from the control input and results in the same fictitious internal rim force in steady state):

$$\tau_{brake}\dot{F}_{x,rim,n} + F_{x,rim,n} = F_{x,control,n} \tag{50}$$

Furthermore, a constant brake force distribution among the axles has to be assumed. It is 7:5:3 for the first, second and third axles respectively. This distribution roughly corresponds to lock of all three axles at 6 m/s^2 brake deceleration in straight line braking.

It is further assumed that the steering actuator (front axle steering only, tag axle steering is not used) is acting on the steering column, therefore the steering ratio and the steering system's compliance has to be additionally compensated by the actuator compared to any other actuating system which directly controls the steering links. Moreover, brake actuator is assumed to be common with the ESP system. Due to lack of data, steering actuator's dynamics is not modelled, i.e. actuation is instantaneous. However, the generation of longitudinal and lateral tyre forces is not instantaneous because of the tyres' longitudinal and lateral relaxation lengths. Finally, both actuators are assumed to be analogue, i.e. they are continuous and they are able to follow the simulation time step.

4.3 Control Algorithm

The vehicle path control for small deviations from the reference (also called desired) path and low lateral acceleration levels could more or less be handled theoretically. There are already some research papers written about it, e.g. Reference [9]. However, in collision avoidance manoeuvres, the lateral displacements and lateral accelerations during the manoeuvre are quite high (close to the stability and handling limits of the

vehicle). This has to be like that in an active safety application, for otherwise the time required for the system to be triggered prior to an impact has to be considerably long. An earlier intervention requires more expensive on-board sensors and complex algorithms to be used in the vehicle since the range of the sensors has to be increased and dynamic traffic situation within this range has to be coped with (Traffic is a dynamic environment, an earlier intervention has to take the possibility of increased number of situation changes ahead of the vehicle into account). As a consequence, these systems have to intervene only at the correct moment. Controlling the vehicle autonomously for a given/desired path at the stability limits requires a little intuition (i.e. without a detailed mathematical control theory) that comes from the deep understanding of the vehicle dynamics and the chassis.

It is assumed that the absolute position and yaw orientation of the vehicle at each time step is known, with an extremely good accuracy using a GPS system (without a GPS system, use of on board sensors only will not suffice in terms of obtaining adequate accuracy, no matter how many advanced estimation techniques are used!). From the Reference [25], it could be seen that a position uncertainty down to ±2 cm is achievable (and this is already available on the market) using today's GPS technology. However, a lesser quality GPS system is assumed, the positioning uncertainties (in terms of standard deviation) are given as follows:

$\sigma_X = 5$ cm

$\sigma_Y = 5$ cm

$\sigma_\psi = 0.5°$

Of course, in order to limit the interference of the noise on the steering wheel (smoother steering intervention is acceptable), a low-pass filter could be used to smoothen the X, Y and ψ position signals. However, extensive care must be taken in the time constant of the low-pass filter (τ_{filter}), as this filter induces time lag and the lag increases when the time constant is increased.

The maximum steering wheel angle that the actuator can reach is limited to 600 degrees for both sides. One reason for that is that at too big steering angles, the steering ratio does not remain constant and therefore the steering angle (wheel angle on the road) will not be determined accurately. 600 degrees (corresponding to approximately 30 degrees of steering angle) is already too big for the "constant steering ratio" assumption to hold. However this limit is kept as it is since there might be a situation where the side slip angle becomes big and sufficiently big countersteer to regain the control of the truck is needed. Another reason to limit the maximum steering angle is that if, for some reason, steering wheel input suddenly becomes too much; then there is a risk of exceeding the adhesion limits and thus reducing the lateral force generation capacity of the front tyres (this is not desired as reduced lateral force generation potential will decrease the path tracking capability at high speeds).

Before explaining the control algorithm, it is important to mention once again that manoeuvrability of a heavy vehicle on a high μ surface is usually limited by the rollover threshold instead of tyres' capability to generate side forces. This fact necessitates path planning in advance in order not to encounter unexpected rollovers.

A simple approach to path planning would be to calculate the longitudinal speed (roughly) and curve radius at each point of a proposed path. By using these, the steady state lateral acceleration can be calculated again at each point and compared with a limit lateral acceleration (a kind of a tuning parameter, e.g. $a_{y,lim}$ = 4.5 m/s^2) and therefore Go/Do not go decision can be made. The following expressions are equivalent of all the explanations given in words:

The steady state lateral acceleration at any point of the reference path:

$$a_{y,ss,ref}(X) = \frac{v_{x,initial}^2 - 2|a_{brake}|S_{ref}(X)}{R_{ref}(X)} \tag{51}$$

where:

$$S_{ref}(X) = \int_{X_i}^{X} \sqrt{1 + \left(\frac{dY_{ref}(X)}{dX}\right)^2}\, dX \quad \text{(path length)} \tag{52}$$

$$R_{ref}(X) = \left(\frac{\frac{d^2 Y_{ref}(X)}{dX^2}}{\left(1 + \left(\frac{dY_{ref}(X)}{dX}\right)^2\right)^{\frac{3}{2}}} \right)^{-1} \quad \text{(curve radius)} \tag{53}$$

and finally, the decision criteria could be given as follows:

$$a_{y,ss,ref}(X) \le a_{y,\lim} \rightarrow YES$$

$$a_{y,ss,ref}(X) > a_{y,\lim} \rightarrow NO$$

The control algorithm is inspired by how a driver drives his/her car. A very rough description of the driving process could be like this: A driver looks ahead, predicts the error based on the difference between current position and the desired position ahead and applies a steering input based on the predicted error. In this thesis, a closed loop control similar to the human driving process is used.

There are different possible control algorithms (all inspired by driving process) with different performance levels.

4.3.1 A P Control Algorithm with No Prediction Feature

It is known that when front axle is controlled to position the vehicle on the road, both yaw orientation and lateral position are adjusted. The control of these two cannot be done independent of each other unless a steerable rear axle is utilised. As a result, the driver also takes this into account and applies an additional correction on the steering

wheel. Based on the ideas listed in this paragraph, the following steering control algorithm can be designed:

$$\delta_{SWA} = K_{p,1}\left(Y_{ref} - Y\right) + K_{p,2}\left(\psi_{ref} - \psi\right) \tag{54}$$

with:

$$Y_{ref} = f(X) \tag{55}$$

$$\psi_{ref} = \arctan\left(\frac{dY_{ref}}{dX}\right) \tag{56}$$

Here, it is assumed that the reference (=desired) path and its mathematical equation with respect to the global longitudinal position (X) are already known.

In the steering control, the second term where the yaw angles are involved has the biggest importance. From an earlier simulation work, it was seen that omission of this second term and use of the first term only results in very large side slip angles and therefore loss of directional stability even though a differential braking intervention to stabilise the vehicle is used (if the CG is high as in the case of the trucks, then usually rollover accident is seen before a full spin-out on when μ is high). Omission of the first term and use of the second term leads to a stable tracking of the reference path, but with a large lateral deviation from the reference path. The good thing with this algorithm (given in Equation 54) and using an accurate GPS system is that the side slip angle is already taken into account by the second term and necessary correction on the steering wheel is automatically made provided that the desired path does not force the vehicle to exceed its stability limits and the path is followed with relatively small lateral deviations (When the path can no longer be followed, then this system will not work efficiently due to incredibly large steering inputs proportional to the tracking error).

A truck, compared to a passenger vehicle, responds slower to the inputs from the driver due to its mass, size and CG height etc. In order to reduce the response times from the truck, a differential braking algorithm is also implemented. This differential braking algorithm is also used to stabilise/steer the truck when the yaw angle and lateral position with respect to the reference path indicates that the vehicle yaw angle is bigger than what is needed. Another advantage of this braking algorithm is that it helps to reduce the longitudinal speed of the vehicle slightly, thus making the vehicle more controllable at a later intervention stage (and because of this, it is active during the whole manoeuvre). However, differential braking has to be approached carefully not to apply too much yaw torque on the vehicle if it is intended to be used to counteract understeer, otherwise the side slip angle of the vehicle increases significantly [26]. An excessive side slip angle will result in loss of control and consequently reduced maximum lateral displacement. Therefore, the control coefficient for differential brake algorithm could be set to a lower value (When the stability is about to be lost, then a lower coefficient could still be sufficient since the automatic steering comes into the action to correct the vehicle). The decided braking algorithm is in the following:

$$F_{x,control,n} = K_{p,brake}\left|\psi_{ref} - \psi\right| \tag{57}$$

However, the wheel ("n") on which the brake force should be applied is decided based on the position of the vehicle and the sign of (ψ_{ref} - ψ). Following figures demonstrate which wheel to brake:

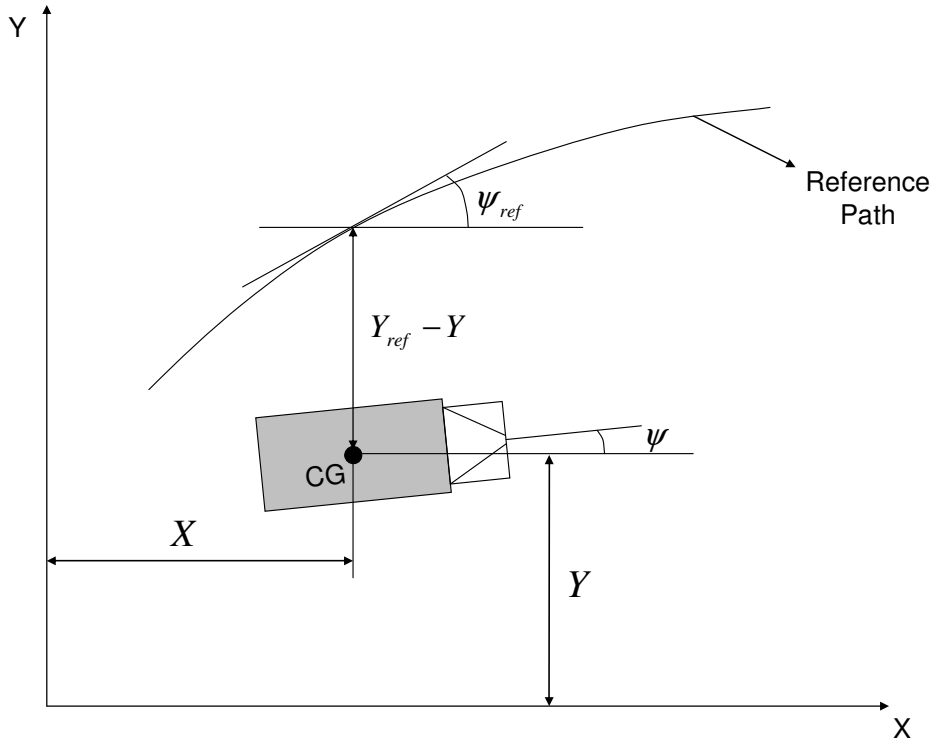

Figure 11 *A generalised figure to depict the variables used in the control algorithm. Possible cases and corresponding wheel to brake is shown in the following figure.*

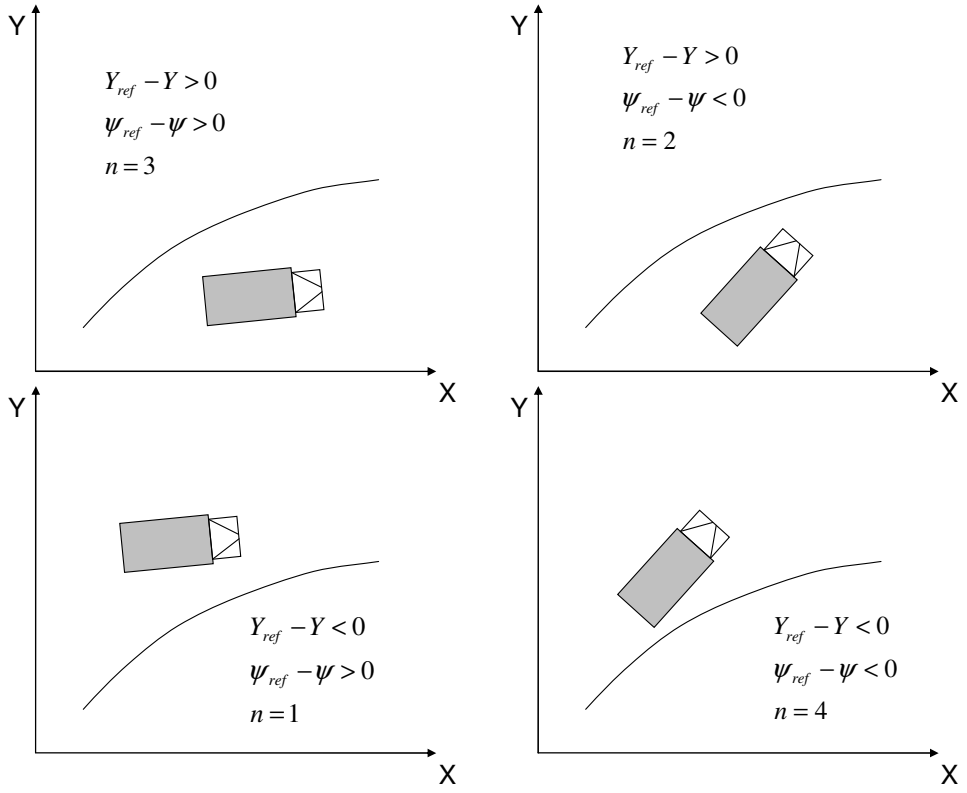

Figure 12 Figure depicting which wheel to brake (shown by "n") depending on the case.

The reason why it is preferred to brake only the one of the wheels on the second axle (n = 3 or 4) instead of braking inner or outer wheels of the second and third axles is that it is always desired to keep some lateral force capacity available at the rear axle. It is known that braking reduces the lateral force generation capacity of a tyre. By not braking any of the wheels on the third axle, there is no doubt that lateral force reserve is increased at the rear compared to the case where the wheels on the second and third axles are braked simultaneously. The reason why a brake actuation on the second axle is preferred to a brake actuation on the third axle is that the second axle's static load is bigger than the third axle's static load. Since the roll damping and roll stiffness coefficients on the second and the third axles are the same; in presence of a load transfer due to cornering, vertical load on the inner wheel of the second axle will be bigger than the vertical load on the third axle. This makes it more difficult to exceed the adhesion limits of the tyre if a brake torque is applied on the inner wheel of the second axle compared to the same brake torque applied on the inner wheel of the third axle.

It is of importance to mention here that the vehicle slows down when differential brake interventions are made. Therefore, if the deceleration is desired to be kept constant in presence of both service braking and differential braking, the differential brake force should be subtracted from the sum of service brake force on all wheels. This means that increased adhesion margin (by reduced brake pressure) on one wheel could be used to get more yaw moment if wheel of interest is already in the limit of adhesion due to service braking (Note that increase in adhesion margin on one

particular wheel depends on the reduced service brake force and the brake force distribution which is assumed to be constant). The "balancing" of differential braking and service braking is realised from the control input. Because of the longitudinal relaxation lengths of the tyres and dynamic response of the brake system, predicted amount of forces/effects will build up later than expected.

4.3.2 Introduction of Prediction Distance and Modified P Control Algorithm

The control strategy explained so far intervenes based on the actual deviation from the reference trajectory. However, this is not an ideal way to control the vehicle travelling at high speeds as a coming or a "future" point has to be taken into account since a control based on the reference point that has "just" passed will not prepare the vehicle for the trajectory ahead because the vehicle response is not instantaneous (Response time for a heavy vehicle is even longer!). Therefore, a "prediction distance", similar to what is given in Reference [27], should be implemented. This means that the reference values should not be based on the actual position of the vehicle, but at a certain distance from it which is ahead of the vehicle. This is also what the driver does while driving: He/she looks ahead and controls the vehicle according to what is coming ahead. As mentioned before, a simplified driving analogy is used in this work. Therefore, additional corrections that arise from the implementation of the "prediction distance" concept should be formulated based on what the driver sees inside the vehicle. The following figure summarises what has been discussed in this paragraph:

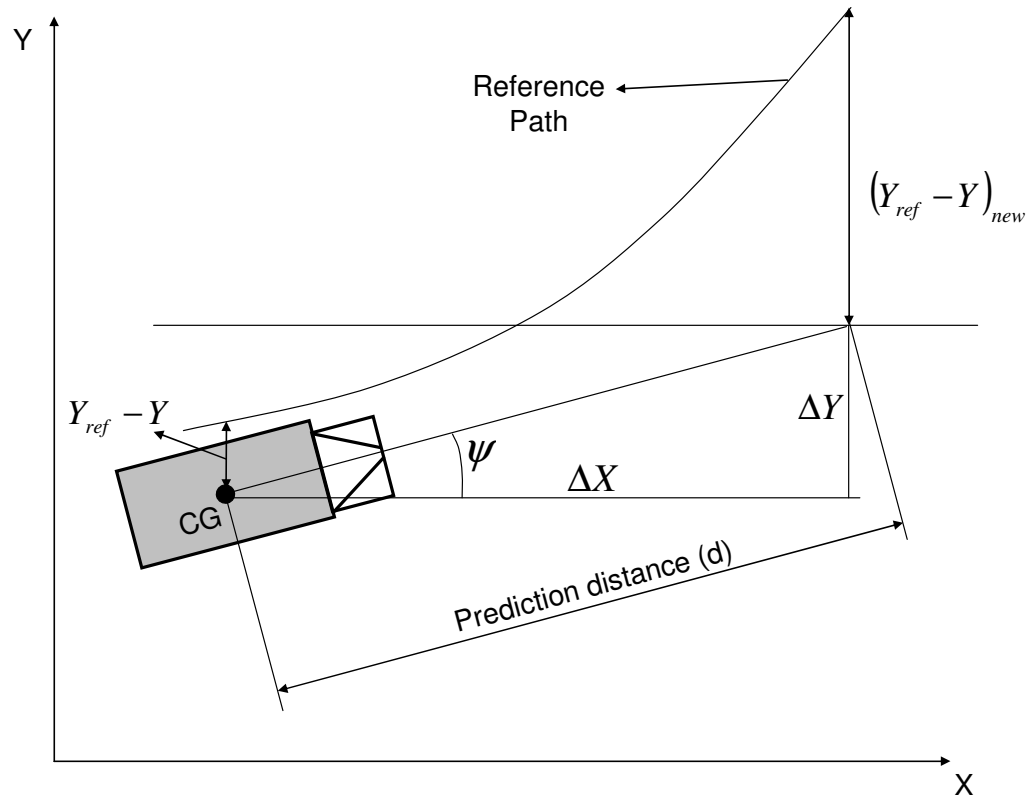

Figure 13 Figure illustrating the "prediction distance" concept

From the Figure 13, it can be seen that:

$$\Delta X = d\cos\psi \tag{58}$$

$$\Delta Y = d\sin\psi \tag{59}$$

The new distance from which the control is applied is then in Equation 60:

$$\left(Y_{ref} - Y\right)_{new} = Y_{ref}\left(X + \Delta X\right) - Y\left(X\right) - \Delta Y \tag{60}$$

The similar approach should be used in yaw angles (or yaw angle error). Since an angle is concerned here, there is no additional term appearing in the equation:

$$\left(\psi_{ref} - \psi\right)_{new} = \psi_{ref}\left(X + \Delta X\right) - \psi\left(X\right) \tag{61}$$

Hence, the control algorithm becomes:

$$\delta_{SWA} = K_{p,1}\left(Y_{ref} - Y\right)_{new} + K_{p,2}\left(\psi_{ref} - \psi\right)_{new} \tag{62}$$

$$F_{x,control,n} = K_{p,brake}\left|\left(\psi_{ref} - \psi\right)_{new}\right| \tag{63}$$

The "prediction distance" concept is not only useful to follow the path much precisely, but also to avoid the rollovers under certain driving conditions. Without the

prediction, when a sharp curve is negotiated, both the lateral displacement and the yaw orientation of the vehicle will remain insufficient in the beginning, thus the control system will demand a big steering angle for a relatively long time period, leading to a rollover accident. However, when the prediction is applied, then the sensed "lack of lateral displacement" at the early stage of the manoeuvre will be reduced due to the small yaw angle already possessed (increase in ΔY term reduces the input steering angle).

Another result that comes from the implementation of the prediction distance is that the yaw correction term becomes obsolete (i.e. $K_{p,2}$ could be set to zero) as the prediction distance is already taking the yaw orientation into account by ΔY term. However, yaw correction term could be kept if the yaw stability of the vehicle is desired to be enhanced in all driving situations (such as on low μ conditions), together with the cost of increased oscillations on the steering input (See simulation results for further details).

It has to be understood that a suitable prediction distance is dependent on the vehicle's longitudinal speed. From the driver analogy, one can say that this prediction distance has to be increased at high speeds since a driver looks further ahead and applies control inputs to the car based on a point that is farther from the vehicle. However, this is not the case for low speed driving. In low speed driving, the prediction distance should be almost zero in order to control the vehicle precisely (Usually, at lower speeds, the manoeuvre involves big yaw angles and lateral displacements and it requires a greater accuracy, such as during parking). A longer prediction distance at low speeds would lead to too much steering inputs and result in unnecessary oscillations. In order to take these concerns into consideration, the following substitution is suggested:

$$d \to d_{ref} \frac{v_x^2}{v_{x,ref}^2} \tag{64}$$

The "reference" values are the ones that are used in the simulation as the initial values ($v_{x,ref} = v_{x,initial} = 80$ km/h, d_{ref} is the prediction distance corresponding to the reference speed). The quadratic form comes from intuition; the question of "how should the most appropriate mathematical form be?" is outside the scope of this thesis (it requires testing the vehicle and the controller behaviour for a large speed span).

In the controller algorithms explained so far, "D" (derivative) control is tried to be avoided and only a "P" (proportional) control is used (instead of a "PD" control). Usually, it is expected that a simpler control algorithm is more robust than a complicated one. Moreover, it will be easier to handle when it comes to the tuning of the control system. Furthermore, a "P" control will require less filtering than a "PD" control as the derivative of a noisy signal from the sensor system of the vehicle cannot be taken with ease (a simple filtering could be used but it will result in a time lag. Time lags are usually unwanted in safety systems! Therefore an advanced filtering may be needed to be used and therefore the complexity of the system increases.). However, the steering control input becomes oscillatory as the vehicle's own yaw damping decreases when the longitudinal speed of the vehicle is increased. Because this is not acceptable (a smooth control input is preferred), use of a PD control

becomes inevitable. The following control algorithm proposes a promising solution to overcome the problem of taking the time derivative of a noisy signal.

4.3.3 A New PD Control Algorithm with Prediction Distance

Recalling Equations 59 and 60:

$$\left(Y_{ref} - Y\right)_{new} = Y_{ref}\left(X + \Delta X\right) - Y\left(X\right) - d\sin\psi \tag{65}$$

Taking the time derivative of the relation:

$$\frac{d\left(Y_{ref} - Y\right)_{new}}{dt} = \frac{dY_{ref}}{dt} - \frac{dY}{dt} - d\cos\psi \cdot \dot{\psi} \tag{66}$$

Using the chain rule:

$$\frac{dY_{ref}}{dt} = \left(\frac{dY_{ref}}{dX}\right)_{X+\Delta X} \frac{dX}{dt} \tag{67}$$

By using the transformations from global coordinate system to local coordinate system, Equations 68 and 69 could be written:

$$\frac{dX}{dt} = v_x \cos\psi - v_y \sin\psi \tag{68}$$

$$\frac{dY}{dt} = v_x \sin\psi + v_y \cos\psi \tag{69}$$

Combining Equations 65, 66, 67, 68 and 69 yield:

$$\begin{aligned}\frac{d\left(Y_{ref} - Y\right)_{new}}{dt} &= \left(\frac{dY_{ref}}{dX}\right)_{X+\Delta X} \cdot \left(v_x \cos\psi - v_y \sin\psi\right) \\ &- \left(v_x \sin\psi + v_y \cos\psi\right) - d\cos\psi \cdot \dot{\psi}\end{aligned} \tag{70}$$

The Equation 70 shows that if vehicle states (longitudinal velocity, lateral velocity and yaw rate) together with the global position and yaw orientation are known, it will be possible to calculate the rate of change in lateral deviation from the desired reference path indirectly. The final (and of course, the better since the oscillations could be reduced) control algorithm becomes:

$$\delta_{SWA} = K_p\left(Y_{ref} - Y\right)_{new} + K_d \frac{d\left(Y_{ref} - Y\right)_{new}}{dt} \tag{71}$$

Note that the yaw correction term is not included since it is no longer needed.

5 Simulation Results

The results will be presented here in two levels: Tuning the controller for a severe manoeuvre and using it for a collision avoidance manoeuvre. For the former case, the initial speed is set to 80 km/h and this is because ISO double lane change manoeuvre is also performed at 80 km/h. For the latter case, speed remains 80 km/h, as this speed fits well to the previous test speed and it is also the one of highest speeds (the more successful results at higher speeds, the more likely the system will be able to track the path precisely at lower speeds) which is frequently seen in the "rear-end collisions due to stopped vehicle in front".

For all the test cases, the lateral deviation at 45^{th} metre (this is where the obstacle is located in X axis; this performance indicator is designed to take the second performance criterion, explained in the problem definition section, into account) and the maximum deviation on the intermediate straight section (this performance criterion is designed to take the third performance criterion, explained in the problem definition section, into account) will be reported in order for the reader to compare the performance when control parameters are varied.

5.1 Tuning and Testing the Controller

For this purpose, the maximum lateral displacement (w) for the manoeuvre is set to 6 m. This value is a little less than the truck can achieve (without wheel lift-off) for the given speed and the reference path as a possible wheel lift-off while testing and tuning the controller for different control coefficients will yield incomparable results.

5.1.1 The P Steering Control with Zero Prediction Distance

As mentioned before, this control requires "balancing" of the lateral displacement with the yaw orientation. A control design that takes only the lateral deviation from the reference (desired) path into account yields to unstable motion of the vehicle.

Setting $K_{p,1} = 2$ and $K_{p,2} = 100$, following result is obtained:

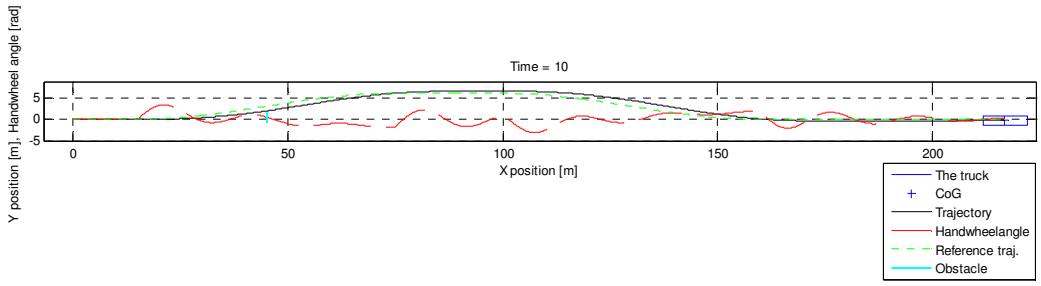

Figure 14 *The path-following result for $K_{p,1}$ = 2, $K_{p,2}$ = 100, $K_{p,brake}$ = 0, K_d = 0, d_{ref} = 0, zero sensor noise, no application of service brakes. Note that axes use the same scale.*

The path deviation at 45th metre is 1.079 m and maximum path deviation on the intermediate section is 0.583 m.

As can be seen, path tracking performance is poor (due to the obvious too big lateral deviations from the reference path) and steering input is oscillatory. This makes it impossible to choose this steering control algorithm.

5.1.2 The P Steering Control with Fixed Prediction Distance and Varied Control Coefficient

Three different output plots are generated for K_p = 20, K_p = 30, K_p = 40 for a fixed d_{ref} = 7 m:

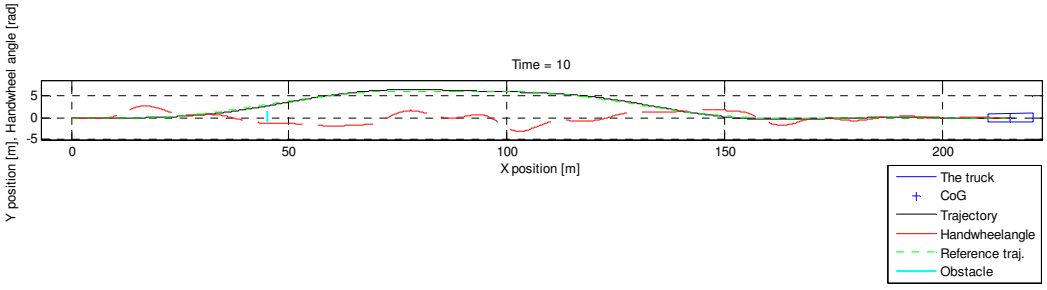

Figure 15 *The path-following result for K_p = 20, $K_{p,brake}$ = 0, K_d = 0, d_{ref} = 7 m, zero sensor noise, no application of service brakes. Note that axes use the same scale.*

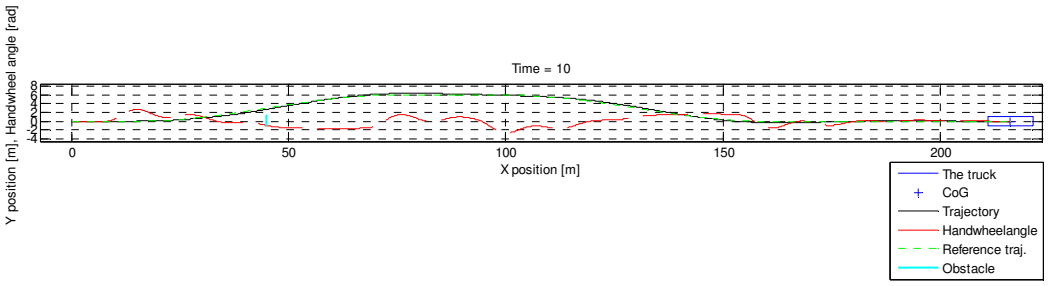

Figure 16 *The path-following result for K_p = 30, $K_{p,brake}$ = 0, K_d = 0, d_{ref} = 7 m, zero sensor noise, no application of service brakes. Note that axes use the same scale.*

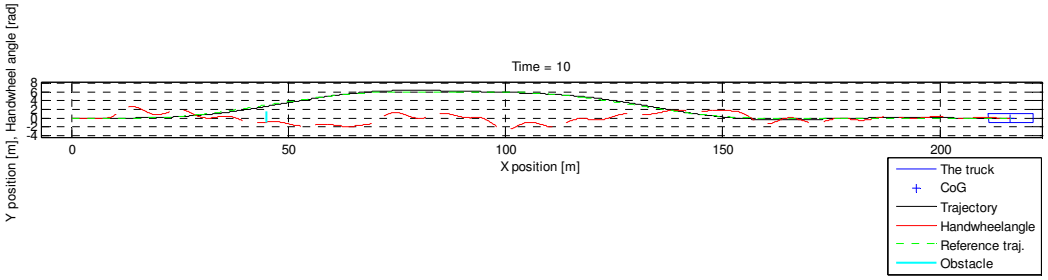

Figure 17 *The path-following result for K_p = 40, $K_{p,brake}$ = 0, K_d = 0, d_{ref} = 7 m, zero sensor noise, no application of service brakes. Note that axes use the same scale.*

Performance evaluation criteria for these three settings are given in Table 2:

Table 2 *The path following performance indicators for $K_{p,brake}$ = 0, K_d = 0, d_{ref} = 7 m, zero sensor noise, no application of service brakes.*

	Path deviation at 45th metre	Max. path deviation on the intermediate straight
For K_p = 20	0.305 m	0.413 m
For K_p = 30	0.296 m	0.397 m
For K_p = 40	0.294 m	0.390 m

As K_p is increased, performance figures are improved, even though improvement is not so significant for the most important performance figure (i.e. path deviation at 45th metre). However, when K_p is set to 40, high frequency (just above 2 Hz) oscillations, which result from inadequate yaw damping (decreases roughly when the speed is increased) of the vehicle at the test speed, occur on the steering wheel input. Because of this, it is not wise to set the K_p to 40; furthermore setting it to 40 does not reduce

the path deviation at 45th metre (which is of higher importance than any other performance indicator) considerably. From this test, it could be concluded that K_p = 30 is the best choice and this value will be used as the fixed parameter for the next test.

It is also worth to say some words on the maximum path deviation on the intermediate straight section. It could be seen that the path deviation values for this region is significantly bigger than the path deviations at 45th metre. The main reason for this is not the vehicle suffering from understeer, but the vehicle going "sideways" (due to sideslip angle) for a very short period of time (It could be seen that controller gives a countersteering input at that instant so as to recover the control of the truck).

5.1.3 The P Steering Control with Fixed Control Coefficient and Varied Prediction Distance

When K_p is set to 30 (kept constant) and three different d_{ref} (6 m which is the lowest possible value without any wheel lifting off the ground for this manoeuvre; 10 m; and 15 m which is the maximum possible value as the initial straight section is 15 m) are used, the following results are obtained:

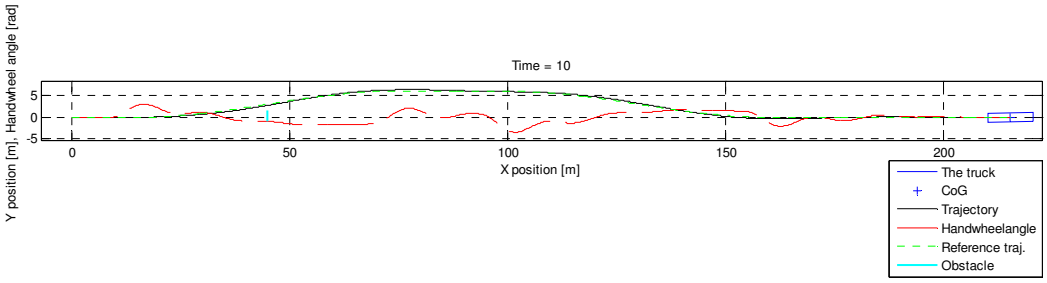

Figure 18 *The path-following result for K_p = 30, $K_{p,brake}$ = 0, K_d = 0, d_{ref} = 6 m, zero sensor noise, no application of service brakes. Note that axes use the same scale.*

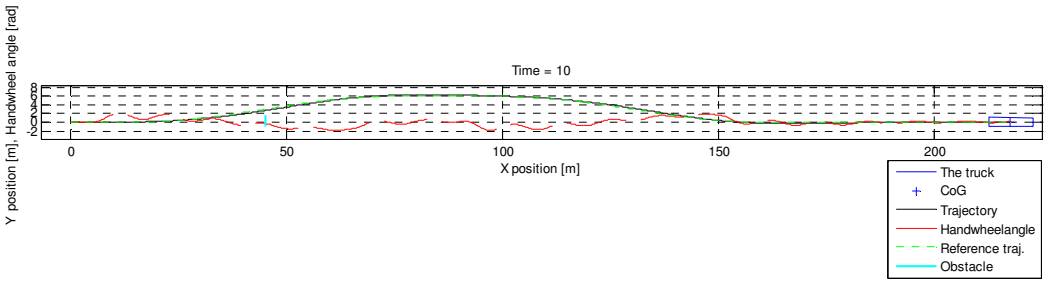

Figure 19 *The path-following result for K_p = 30, $K_{p,brake}$ = 0, K_d = 0, d_{ref} = 10 m, zero sensor noise, no application of service brakes. Note that axes use the same scale.*

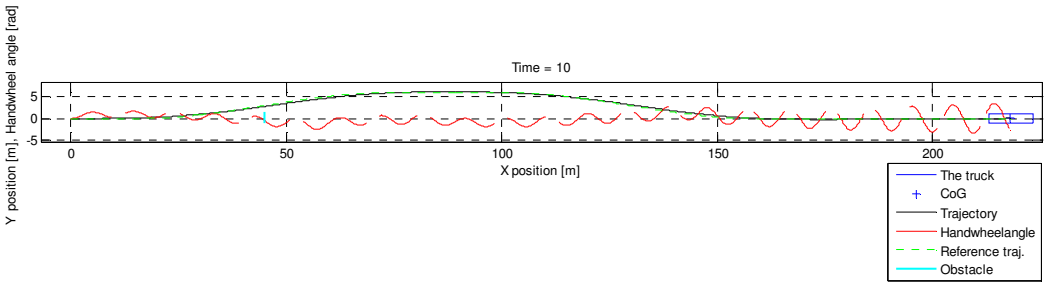

Figure 20 *The path-following result for K_p = 30, $K_{p,brake}$ = 0, K_d = 0, d_{ref} = 15 m, zero sensor noise, no application of service brakes. Note that axes use the same scale.*

Performance evaluation criteria for these three settings are given in the following Table 3:

Table 3 *The path following performance indicators for K_p = 40, $K_{p,brake}$ = 0, K_d = 0, zero sensor noise, no application of service brakes.*

	Path deviation at 45th metre	Max. path deviation on the intermediate straight
For d_{ref} = 6 m	0.273 m	0.373 m
For d_{ref} = 10 m	0.312 m	0.363 m
For d_{ref} = 15 m	0.220 m	0.231 m

As d_{ref} is increased, maximum path deviation on the straight section decreases. This is not surprising since increase of d_{ref} adds more prediction to the controller and therefore the intermediate straight section is recognised much earlier. Steering input is provided much smoother (and this leads to reduced sideslip angle in the beginning of the intermediate straight section), however this causes the path deviation to increase in between 45th and 70th metres since too long prediction distances cause the reference points in the vicinity of the vehicle to be missed. Shorter prediction distances are usually beneficial in order to improve the path tracking performance at all points of the desired path. However, when the result for d_{ref} = 15 m is observed, it could be seen that path deviation at 45th metre is significantly lower than the test cases with shorter d_{ref}. This exception is caused by the initial 15 m of straight section to be used for getting a lateral displacement even if the reference path section remains straight. The lateral displacement achieved here contributes to the lateral displacement at 45th metre and improves it even though the path tracking performance decreases.

Another important point here is that increased d_{ref} results in oscillatory steering input from the controller. This is because it acts like a "lever arm" which increases the path deviation, therefore the control input becomes bigger (therefore it acts in the same way as increased K_p in that sense). A big control input results in oscillatory motion

(again, because of lack of yaw damping) and instability on the final straight section (steering input gets bigger and bigger instead of getting damped when d_{ref} is set to 15).

From the results obtained from this section, one could conclude that d_{ref} should be kept as short as possible (not too short though, otherwise it will result in rollovers) in order to obtain the best path tracking performance. Because d_{ref} = 6 m is already on the limit of the wheel lift-off (close to rollover), it is preferred to keep d_{ref} = 7 m which is the same as in the previous chapter.

5.1.4 The PD Steering Control with Fixed Prediction Distance and Varied Control Coefficients

Firstly, the effect of K_d on the control and control performance will be shown. The other control parameters are kept the same:

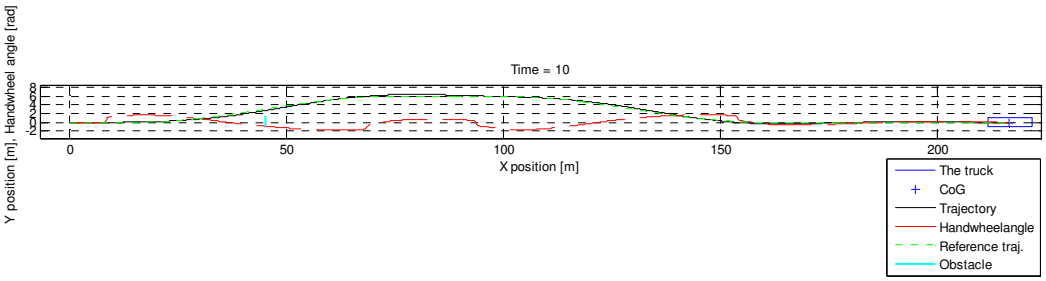

Figure 21 *The path-following result for K_p = 30, $K_{p,brake}$ = 0, K_d = 10, d_{ref} = 7 m, zero sensor noise, no application of service brakes. Note that axes use the same scale.*

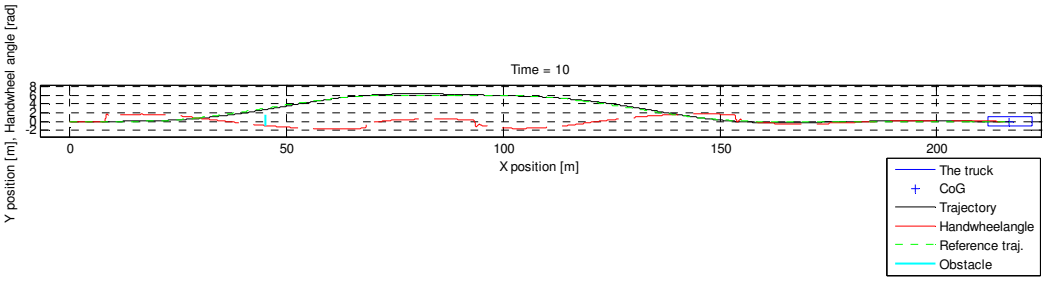

Figure 22 *The path-following result for K_p = 30, $K_{p,brake}$ = 0, K_d = 30, d_{ref} = 7 m, zero sensor noise, no application of service brakes. Note that axes use the same scale.*

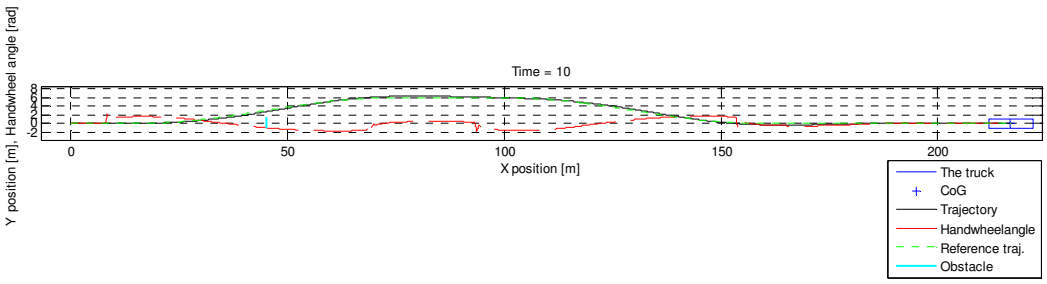

Figure 23 *The path-following result for K_p = 30, $K_{p,brake}$ = 0, K_d = 50, d_{ref} = 7 m, zero sensor noise, no application of service brakes. Note that axes use the same scale.*

Performance evaluation criteria for these three settings are given in Table 4:

Table 4 *The path following performance indicators for K_p = 30, $K_{p,brake}$ = 0, d_{ref} = 7 m, zero sensor noise, no application of service brakes.*

	Path deviation at 45th metre	Max. path deviation on the intermediate straight
For K_d = 10	0.309 m	0.405 m
For K_d = 30	0.300 m	0.384 m
For K_d = 50	0.292 m	0.373 m

As could be seen from the results, steering oscillations have disappeared as expected. Furthermore, it could be seen that steering input settles down to zero quicker on the last straight section as K_d increases. This reveals that the lack of yaw damping is no longer a problem with this control algorithm, moreover handing the control to the driver after the autonomous intervention could be performed smoother.

From the linear control theory, it is known that increased proportional control coefficient reduces the rise time for the system (especially a second order system, which is similar to the linearised vehicle), usually at the cost of increased oscillations, overshoots and possible instabilities. However; if a PD control is utilised, those problems are expected to be solved. Here, because differential control (="D" effect) is implemented; it is of interest to investigate how the system will behave for bigger K_p coefficients. Figures 24 and 25 demonstrate this for a fixed K_d:

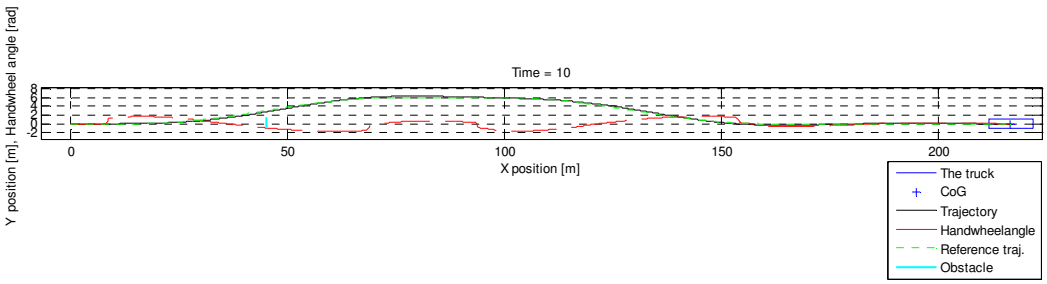

Figure 24 *The path-following result for K_p = 60, $K_{p,brake}$ = 0, K_d = 10, d_{ref} = 7 m, zero sensor noise, no application of service brakes. Note that axes use the same scale.*

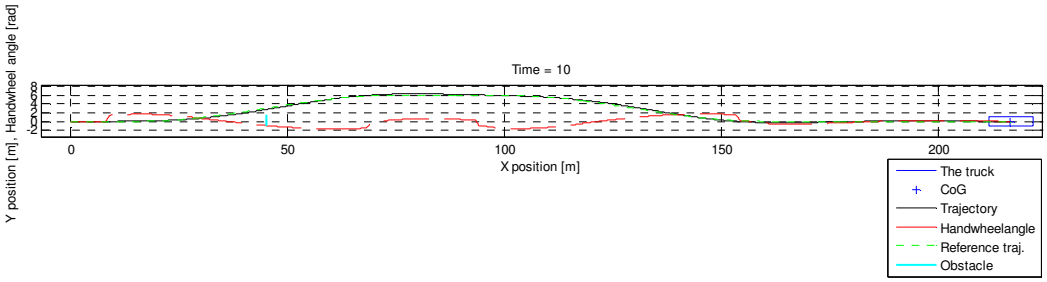

Figure 25 *The path-following result for Kp = 90, Kp,brake = 0, Kd = 10, dref = 7 m, zero sensor noise, no application of service brakes. Note that axes use the same scale.*

Performance evaluation criteria for these two settings are given in Table 5:

Table 5 *The path following performance indicators for K_d = 10, $K_{p,brake}$ = 0, d_{ref} = 7 m, zero sensor noise, no application of service brakes.*

	Path deviation at 45th metre	Max. path deviation on the intermediate straight
For K_p = 60	0.293 m	0.380 m
For K_p = 90	0.289 m	0.372 m

It could be seen from the results that further increase of K_p does not result in considerable improvement in path following performance indicators. This means that K_p could be limited to 90, as further increase in this gain is expected to lead to supply of noisy steering input to the steering actuator when "positioning sensor noise" is utilised in the simulation.

To sum up, K_p = 90 and K_d = 10 are two coefficients that are found to perform well and thus they will be kept constant for the simulations whose results will be provided onwards.

5.1.5 The P Differential Brake Control with Varied Control Coefficient Using the Current Steering Algorithm

The effect of the differential brake so as to improve the path following is depicted as follows:

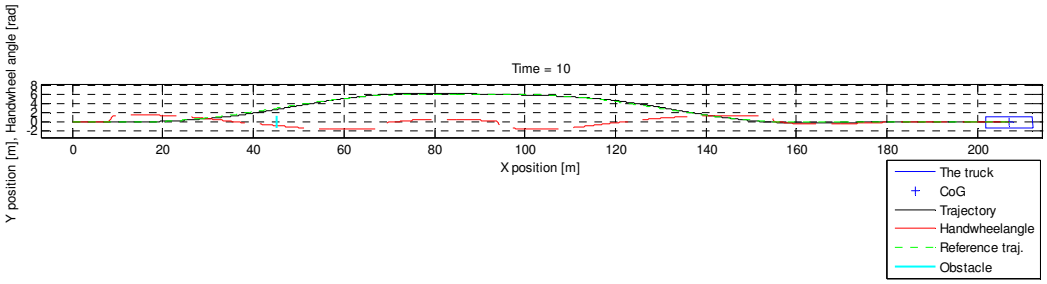

Figure 26 *The path-following result for K_p = 90, $K_{p,brake}$ = 200000, K_d = 10, d_{ref} = 7 m, zero sensor noise, no application of service brakes. Note that axes use the same scale.*

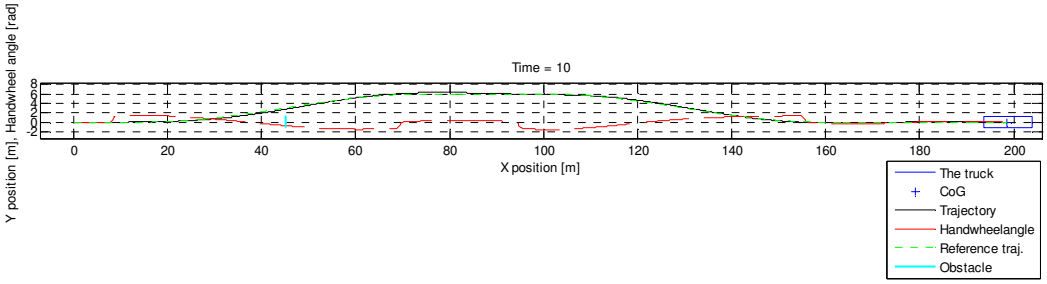

Figure 27 *The path-following result for K_p = 90, $K_{p,brake}$ = 400000, K_d = 10, d_{ref} = 7 m, zero sensor noise, no application of service brakes. Note that axes use the same scale.*

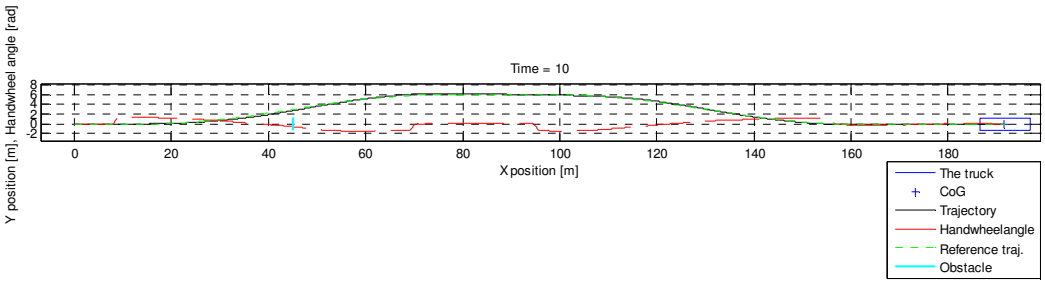

Figure 28 *The path-following result for K_p = 90, $K_{p,brake}$ = 600000, K_d = 10, d_{ref} = 7 m, zero sensor noise, no application of service brakes. Note that axes use the same scale.*

Performance evaluation criteria for these three settings are given in Table 6:

Table 6 *The path following performance indicators for K_p = 90, K_d = 10, d_{ref} = 7 m, zero sensor noise, no application of service brakes.*

	Path deviation at 45th metre	Max. path deviation on the intermediate straight
For $K_{p,brake}$ = 200000	0.280 m	0.340 m
For $K_{p,brake}$ = 400000	0.273 m	0.307 m
For $K_{p,brake}$ = 600000	0.265 m	0.273 m

As could be seen, the continuously applied differential brake actuation makes it possible to reduce the path deviation at 45th metre slightly, but the most important effect of it is on the maximum path deviation on the intermediate straight section.

The improved results is not only because of the provision of a correcting yaw torque (which has the biggest effect especially on the vehicle motion on the intermediate straight section as it acts as a stability control to reduce the sideslip angle), but also due to the reduction of speed when any of the wheels is braked.

From the results, it could be seen that increased $K_{p,brake}$ yields to good results. However, if the intervention here is too aggressive, it will result in the full range of adhesion to be used, thus leaving no room for that wheel to be useful for service braking. Moreover, from the previous simulations (not shown here), it was seen that too high $K_{p,brake}$ did not yield significantly improved path following performance as the current controller already behaves satisfactorily. Therefore, the control coefficient could be kept limited. This strategy is particularly beneficial in restricting the side slip angles on low μ surfaces and reducing the brake disc and lining wear. As a result, $K_{p,brake}$ = 600000 could be selected for further simulations.

5.2 Using the Controller for Collision Avoidance Application

For this application, the maximum lateral deviation is set to w = 6.8 m (therefore targeted lateral displacement in the vicinity of the obstacle is 3.4 m). This is because:

- Right edge of the obstacle (which has a width of 2.6 m) in front is aligned with the right edge of the truck, this means that CG of the truck should move at least 2.6 m laterally.

- The controller acts according to the lateral deviations. 0.4…0.5 m lateral deviation (these values are similar to the lateral deviations which has been observed in the tuning of the controller, moreover the positioning noise also has to be taken into account!) from the path has to be taken into account as the truck cannot follow the desired path without any lateral deviation.

- The distance from the CG to the rearmost point of the truck is considerably long. This means that truck's yaw motion will cause rear-end of the truck to move towards the obstacle. Thus, the remaining margin is left in order to avoid a possible side swipe with the obstacle.

Note that these values are valid for the concerned path, initial speed and road conditions! Change of road conditions (e.g. reduction in the maximum adhesion that could be exploited from the road), initial speed and form of the path will require different assumptions for the given values.

It is also worth to note that the front right corner of the truck reaches the obstacle first and when this happens, the targeted lateral deviation for the CG does not even reach 3.4 m (because of the distance between the CG and the frontmost point of the truck). However, the lack of lateral displacement is approximately offset by the yaw motion of the vehicle (so the front right corner attains sufficient lateral displacement); therefore this does not create too many problems for this type of path.

In order for the steering (or steering + braking) intervention to be favourable compared to pure braking, it is of importance to know roughly the braking distance for the truck on high μ road conditions. Assuming that a real truck could reach an average brake deceleration of 7 m/s^2, the distance required to stop while travelling at 80 km/h is:

$$\frac{v_{x,initial}^2}{2|a_x|} = \frac{(80/3.6)^2}{2|-7|} = 35.3 \text{ m} \tag{72}$$

Hence, the steering intervention should be able to provide adequate lateral displacement in about 35 m (again, on high μ!). If this is not possible, one should not design a steering intervention that is trying to steer the truck away from the obstacle as a lot of uncertainties around the vehicle has to be handled carefully (road edge, oncoming traffic, traffic coming from behind etc.) when the steering intervention is the case.

There is one other issue with the steering intervention to be taken into account; that is the prediction distance! Actually, steering intervention starts before the sinusoidal section is reached (because of the prediction distance). Since this is the case, then it means that the vehicle's sensing system has already detected the obstacle a little in advance; therefore one could think that the system could have initiated a full braking just at the time when the steering intervention was intended to be started (in other words, braking could have been performed a little in advance as well, again because of the prediction distance). This imposes a restriction on the maximum prediction distance to be used for this study. A very simple and approximate analysis reveals that for this given path (demanding 3.4 m of lateral displacement for the CG in 30 m), the initial prediction distance determined by d_{ref} should not be longer than 10 m for the steering (or the combination of steering and braking) intervention to remain advantageous compared to pure braking (assuming that the brake-to-stop distance is approximately 35 m as calculated) since there is roughly 5 m (l_1 + fo) of distance between the CG and the frontmost point of the vehicle.

In this section, noise on the positioning system and corresponding low-pass filtering (time constant τ_{filter} = 0.1 s) is enabled in order to improve the realism of the simulation. However, during the first trials, it was found that d_{ref} = 7 m (which was decided in the "tuning/testing of the controller" section) was not sufficient for the truck to negotiate the path without any wheel lifting off the ground. This is caused by the inevitable time lag from the low pass filter, i.e. the measured position values are fed back to the control system with a delay. One way to solve this problem is to increase the prediction distance (delay is compensated by the increase in the prediction distance). Therefore, d_{ref} had to be increased to 8.5 m for this section.

Here; because of the extreme nature of the desired path, the vehicle is unable to complete the manoeuvre without wheel lift off (even with the differential braking intervention). This means that service brakes have to be applied in order to reduce the speed while the path following is in progress. Various open loop application of the service brakes are given in Figures 29, 30, 31:

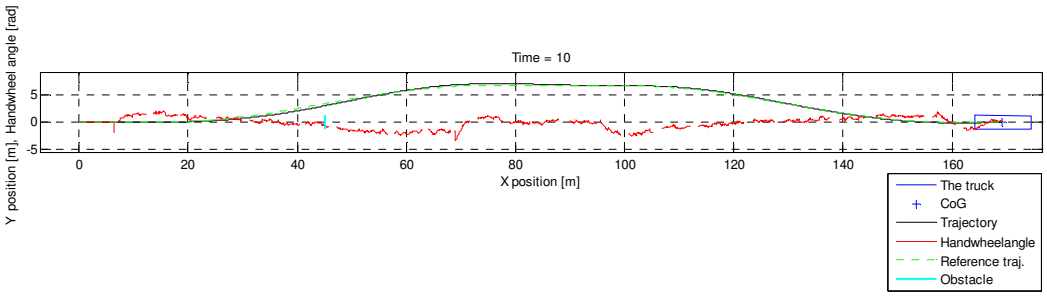

Figure 29 *The path-following result for K_p = 90, $K_{p,brake}$ = 600000, K_d = 10, d_{ref} = 8.5 m, sensor noise on the positioning system enabled (low-pass filter's time constant is 0.1), service brake application corresponding to approximately 1 m/s^2 deceleration on a straight road. Vehicle is able to avoid the obstacle here. Note that axes use the same scale.*

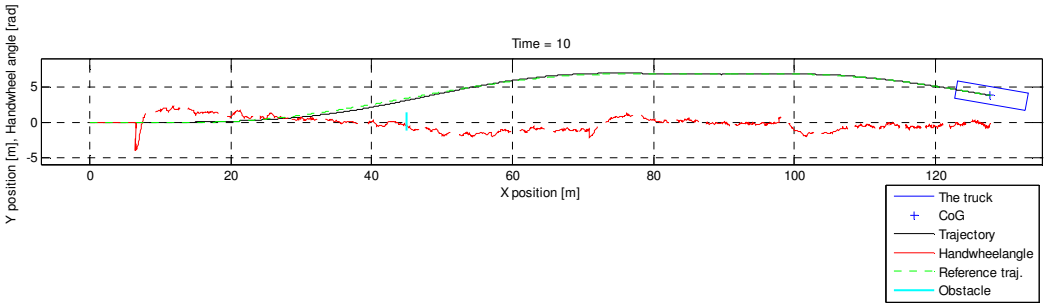

Figure 30 *The path-following result for K_p = 90, $K_{p,brake}$ = 600000, Kd = 10, d_{ref} = 8.5 m, sensor noise on the positioning system enabled (low-pass filter's time constant is 0.1), service brake application corresponding to approximately 2 m/s^2 deceleration on a straight road. Vehicle is able to avoid the obstacle here. Note that axes use the same scale.*

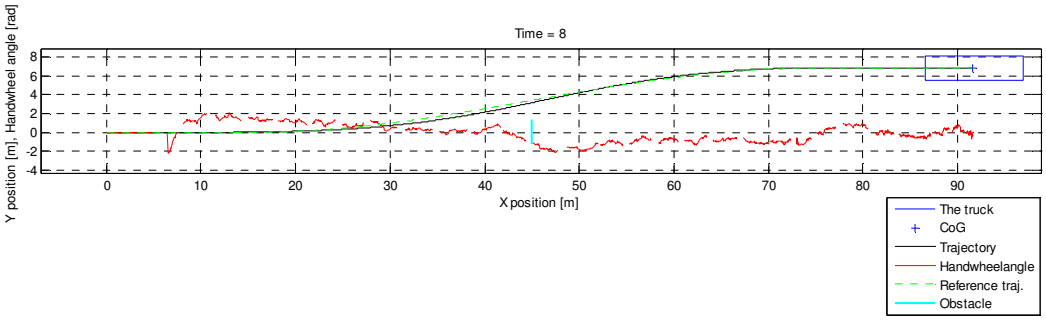

Figure 31 *The path-following result for K_p = 90, $K_{p,brake}$ = 600000, K_d = 10, d_{ref} = 8.5 m, sensor noise on the positioning system enabled (low-pass filter's time constant is 0.1), service brake application corresponding to approximately 3 m/s^2 deceleration on a straight road. Vehicle is able to avoid the obstacle here. Note that axes use the same scale and the vehicle stops in the end of the simulation.*

Performance evaluation criteria for these three settings are given in Table 7:

Table 7 *The path-following result for K_p = 90, $K_{p,brake}$ = 600000, K_d = 10, d_{ref} = 8.5 m, sensor noise on the postioning system enabled (low-pass filter's time constant is 0.1). For all the cases, the truck can avoid the obstacle without hitting it frontally or side swiping.*

	Path deviation at 45th metre	Max. path deviation on the intermediate straight
For 1 m/s^2 deceleration	0.370 m	0.318 m
For 2 m/s^2 deceleration	0.312 m	0.139 m
For 3 m/s^2 deceleration	0.227 m	0.027 m

From the results, it could be seen that application of "soft" service braking (depending on the surface condition and the brake force distribution) while performing the swerve helps the vehicle to keep the desired path in a more successful manner, even though this is not intuitively obvious as the side force capacity for the tyres declines in presence of longitudinal forces. This result reveals the importance of speed reduction in critical manoeuvres (provided that the braking is not harsh so that the front axle is able to steer the vehicle adequately).

6 Conclusion

To sum up, following conclusions could be drawn:

- An accurate global positioning system (not necessarily a system which is only the satellite based) and a good-enough path planning are needed for path tracking applications in heavy vehicles that are intended for severe collision avoidance manoeuvres.

- The best P steering controller among the ones tested is the one with the prediction distance. Without the prediction distance, it is almost impossible to keep the lateral deviations minimal especially at high speeds.

- The longer the prediction distance is, the smoother the steering intervention gets. This means that the vehicle will less likely rollover. However, in order to keep the vehicle (or CG of the vehicle) on the desired escape path with minimal lateral deviations, then shorter prediction distances (but not too short too cause any directional instabilities and rollovers) are preferable. Moreover, shorter prediction distances should be preferred when the initial driving speeds are low and it is desired not to amplify P steering controller coefficient too much.

- In order to limit the amplitudes of steering oscillations (since the yaw damping decreases for the vehicle at high speeds) to avoid a busy intervention and to make it easier to hand the control over the driver, a PD steering controller has to be used. This could be realised only with a P steering controller hardware if the longitudinal speed, lateral speed and yaw rate signals are reliable. This method also makes it possible to obtain the derivative of a digital lateral deviation signal without too many problems.

- A continuous (provided that the system usage is limited and only for a short period of time) differential brake control throughout the manoeuvre not only improves the path tracking and path stability, but also increases the safety by reducing the vehicle speed slightly.

- The negative effect of time lag on path following performance, caused by low-pass filtering of the position signals, could be overcome to a great extent by increasing the prediction distance.

- In order for the path control system to be advantageous over the pure service braking in collision avoidance manoeuvres, a combination of closed-loop path control application and open-loop service braking may be needed. Provided that the service braking is "soft" for the surface conditions (e.g. corresponding to maximum 3 m/s^2 deceleration for a maximum adhesion coefficient of 0.8-0.9), the path following performance increases or at least becomes reasonable if the path is too severe for the truck to handle.

7 Recommendations for Future Work

Because this study cannot cover all the aspects of a collision avoidance system, there are some future work left for further studies. They are given in the following:

- **A way to find a cheaper but yet an accurate positioning system:** A very accurate global positioning system is needed for the controller proposed in the study. The reason why this is needed is that the maximum lateral acceleration the truck can reach is usually limited by the rollover threshold on a high mu surface, not by the tyre forces. As a consequence, the desired escape path should be planned in advance and made sure that the rollover threshold will not be exceeded in the collision avoidance manoeuvre. In addition to this, tight control with high gains and reduced lateral path deviations is a necessity (and this also requires accurate positioning system) since this is the way to keep the steering angles limited (to avoid rollovers when the lateral deviations increase very fast and the controller outputs a bigger steering angle to reduce it) and the lateral deviations from the desired path minimal. A satellite based global positioning system which fits to this application is already commercially available at a high cost. However, instead of using this system, a cheaper GPS system could be fused with environmental sensors such as RADAR, LIDAR etc. to improve the accuracy provided that required accuracy level is feasible.

- **Issues about the robustness of the control system:** The robustness of the control system has to be verified (because it has to handle complex driving conditions and rapidly changing environment) even though it is expected that the proposed control algorithm is robust as it is simple, involves closed loop control and does not include any vehicle model (whose parameters are subject to changes) running inside.

- **Legal issues:** Because autonomous driving is involved; legislations and legal cases, where it is claimed for example that the vehicle has autonomously steered itself off the road, should be considered in detail.

- **Issues about driver acceptance and adoption:** Human drivers are always reluctant about a system that takes the whole control away from the driver. This prevents the system to penetrate into the market thoroughly, therefore has to be taken into account.

- **Overridability issues:** The system has to react fast in the beginning, as could be seen from the results presented in this study. A driver whose hands are on the steering wheel may likely be injured when this type of intervention is concerned; apart from it, any moment applied on the steering wheel inadvertently (since the drivers hand are on the steering wheel) when the fast intervention is initiated will override the system and lead to poor path following performance. One solution to this is to decouple the steering column from the recirculating ball steering gearbox by means of a clutch; however this solution will make the realisation of overridability impossible or very difficult. Therefore this issue has to be investigated in the future.

- **Issues about the vehicle model and chassis data:** Vehicle models and chassis data that are used for simulating the evasive collision avoidance manoeuvres should be as realistic as possible because the result is either "collision" or "no collision", hence every centimetre and decimetre count! Therefore the results obtained in this thesis should be compared with a more accurate vehicle model. This will also help reducing the amount of real-life testing of the control system.

- **Issues about the control algorithm:** In this study, a simple control algorithm for path following purposes is presented. The question here is whether a more advanced (e.g. model predictive control) control algorithm will provide better results or not, this could be answered in the proceeding studies.

- **Issues about the predefined static path:** Because the traffic is a highly dynamic complex environment, predefinition of a static path that is going to be used for a collision avoidance manoeuvre is not always possible. It may be required, depending on the situation, to alter the desired reference path because of oncoming traffic, traffic coming from behind, an obstacle which is located on the reference path and not detected while the reference path is being calculated etc. Dynamic path following needs to be studied in the future.

8 References

1. Pettersson, H. E. (2009): Human Behaviour and Traffic Safety. Lecture notes in TME105 Human Aspects of Traffic Safety Course at Chalmers University of Technology. Göteborg, Sweden.

2. Wismans, J. (2009): Introduction in Integrated Vehicle Safety. Lecture notes in MMF320 Active Safety Course at Chalmers University of Technology. Göteborg, Sweden.

3. Lie, A. (2009): Lecture notes in MMF320 Active Safety Course at Chalmers University of Technology. Göteborg, Sweden.

4. van Zanten, A. T. (2000): Bosch ESP Systems: 5 Years of Experience. SAE International Paper 2000-01-1633, May 2000.

5. Lane Departure Prevention by Nissan. http://www.nissan-global.com/EN/TECHNOLOGY/INTRODUCTION/DETAILS/LDP/

6. Hulthén, J. (2008): Lecture notes in TME120 Introduction to Automotive Engineering Course at Chalmers University of Technology. Göteborg, Sweden.

7. Matschinsky, W. (2000): *Road Vehicle Suspensions (Translation from German to English Edited By Alan Baker)*. Professional Engineering Publishing, Bury St Edmunds, Suffolk.

8. Gerdes, J. C., Rossetter, E. J. (1999): A Unified Approach to Driver Assistance Systems Based on Artificial Potential Fields. *Proceedings of ASME International Mechanical Engineering Congress and Exposition*, November 1999, Nashville, Tennessee.

9. Hiraoka, T., Nishihara, O., Kumamoto, H. (2009): Automatic Path-Tracking Controller of a Four-Wheel Steering Vehicle. *Vehicle System Dynamics*, Vol. 47, No. 10, October 2009, pp. 1205-1207.

10. Thommyppillai, M., Evangelou, S., Sharp, R. S. (2009): Car Driving at the Limit by Adaptive Linear Optimal Preview Control. *Vehicle System Dynamics*, Vol. 47, No. 12, December 2009, pp. 1535-1550.

11. European Truck Accident Causation (ETAC) Study: Full Report.

12. Pacejka, H. B. (2006): *Tyre and Vehicle Dynamics*. Elsevier, Jordan Hill, Oxford.

13. Wong, J. Y. (2001): *Theory of Ground Vehicles*. John Wiley & Sons, New York.

14. International Transport Forum (2010): Permissible Maximum Weights in Europe (Technical data sheet for maximum axle weights). Retrieved: http://www.internationaltransportforum.org/europe/road/pdf/weights.pdf

15. Volvo Trucks FH 62R B3LH1 Data Sheet.
Retrieved: http://datasheets.volvotrucks.com/getfile.aspx?id=1024408

16. Klomp, M. (2007): *On Drive Force Distribution and Road Vehicle Handling – A Study of Understeer and Lateral Grip*. Licentiate Thesis. Department of Applied Mechanics, Chalmers University of Technology, Publication no. 2007:12, Göteborg.

17. Milliken, W. F., Milliken, D. L. (1994): *Race Car Vehicle Dynamics*. SAE International.

18. Ahmed, H. S. T., Yarmohamadi, H. (2006): *Active Rear Wheel Steering of Heavy Vehicles – Applied to a 6X2 Volvo Truck*. Master's Thesis. Department of Applied Mechanics, Chalmers University of Technology, Publication no. 2006:22, Göteborg.

19. Fancher, P., Bernard, J., Clover, C., Winkler, C. (1997): Representing Truck Tire Characteristics in Simulations of Braking and Braking-in-a-Turn Maneuvers. *Vehicle System Dynamics*, Vol. 27, No. 1, pp. 207-210.

20. Heisler, H. (2002): *Advanced Vehicle Technology*. Elsevier, Jordan Hill, Oxford.

21. Mercedes-Benz Türk's website: Illustrative photo of a Mercedes-Benz Axor Truck's tandem axle. http://www.mercedes-benz.com.tr/content/turkey/mpc/mpc_turkey_website/tr/home_mpc/truck_home/home/trucks/axor/chassis.fb0003.html

22. Kharrazi, S. (2009): Simplified Analysis of Steady State Cornering of Heavy Vehicles. Lecture notes in TME100 Advanced Vehicle Dynamics Course at Chalmers University of Technology. Göteborg, Sweden.

23. Aurell J. (September 2010): Personal communication.

24. Göktan, A. G., Güney, A., Ereke, M. (1995): *Taşıt Frenleri* (Road Vehicle Brake Systems. In Turkish), AlliedSignal Automotive, Istanbul, 107 pp.

25. Anthony Best Dynamics' website: In-vehicle Robots. http://www.abd.uk.com/categories.php?Cat=85&PageTitle=In-vehicle Robots

26. Klomp, M (2010): *Longitudinal Force Distribution and Road Vehicle Handling*. PhD Thesis. Department of Applied Mechanics, Chalmers University of Technology, Göteborg.

27. Genta, G. (1997): *Motor Vehicle Dynamics: Modelling and Simulation*. World Scientific Publishing, Singapore.

28. Khodabakshian, M. (2009): *Vehicle Stability Control By Augmenting Brake Control and Active Steering – Applied to a 6X2 Volvo Truck*. Master's Thesis. Department of Applied Mechanics, Chalmers University of Technology, Publication no. 2009:28, Göteborg.

29. Liang, W., Medanic, J., Ruhl, R. (2008): Analytical Dynamic Tire Model. *Vehicle System Dynamics*, Vol. 46, No. 3, March 2008, pp. 197-227.

9 Appendix

9.1 Vehicle data

Note: Some of the vehicle data given below could also be encountered in "Modelling of a Heavy Truck" section since there was a need for motivating how the numerical values of missing tyre/vehicle parameters were assumed. Some of the data given below may be valid for a limited range.

$\mu_{1,i=1,2,3}$	0.85	[-]
$\mu_{2,1}$	$\frac{0.1}{7000 \cdot 9.81}$	[N^{-1}]
$\mu_{2,2}$	$\frac{0.1}{5750 \cdot 9.81}$	[N^{-1}]
$\mu_{2,3}$	$\frac{0.1}{7500 \cdot 9.81}$	[N^{-1}]
$C_{1,i=1,2,3}$	-2.10^{-5}	[N^{-1}.rad^{-1}]
$C_{2,1}$	5.8614	[rad^{-1}]
$C_{2,i=2,3}$	6.515	[rad^{-1}]
$F_{y,a,n} \diagup D_n$	0.75	
$\alpha_{m,n=1,2}$	$\left(10 + \frac{5}{7500 \cdot 9.81} F_{z,n}\right) \frac{\pi}{180}$	[rad]
$\alpha_{m,n=3,4}$	$\left(10 + \frac{5}{5750 \cdot 9.81} F_{z,n}\right) \frac{\pi}{180}$	[rad]
$\alpha_{m,n=5,6}$	$\left(10 + \frac{5}{7000 \cdot 9.81} F_{z,n}\right) \frac{\pi}{180}$	[rad]
$\sigma_{x,n=1...6}$	0.2	[m]
$\sigma_{y,n=1...6}$	0.4	[m]
m	26000	[kg]
m_{unspr}	2500	[kg]
I_{xx}	19000	[kg.m^2]
I_{zz}	150000	[kg.m^2]
g	9.81	[kg.m.s^{-2}]
L	4.900	[m]
BS	1.370	[m]
L_t	5.441	[m]
l_1	3.976	[m]
B	2.050	[m]
$B_{\max}$	2.495	[m]
$L_{\max}$	10.305	[m]
fo	1.360	[m]

$F_{z,n=1,2}$	$3500g$	[N]	
$F_{z,n=3,4}$	$5750g$	[N]	(total wheel load for dual wheel system)
$F_{z,n=5,6}$	$3750g$	[N]	
h'	0.9	[m]	
h_1	0.3	[m]	
$h_{i=2,3}$	0.8	[m]	
K_ϕ	1540000	[N.m.rad^{-1}]	
$K_{\phi,1}$	380000	[N.m.rad^{-1}]	
$K_{\phi,i=2,3}$	580000	[N.m.rad^{-1}]	
C_ϕ	86000	[N.m.s.rad^{-1}]	
$C_{\phi,1}$	28000	[N.m.s.rad^{-1}]	
$C_{\phi,i=2,3}$	29000	[N.m.s.rad^{-1}]	
c_δ	$4.88 \cdot 10^{-7}$	[rad.N^{-1}]	
$\varepsilon_{n=1,2}$	0.14	[-]	(Deflection towards toe-in is assigned to be for a positive roll angle)
$\varepsilon_{n=3,4}$	-0.10	[-]	
$\varepsilon_{n=5,6}$	-0.10	[-]	
σ_{brake}	0.1	[s]	
i_s	20	[-]	